Engineering Structures 250 (2022) 113391

Contents lists available at ScienceDirect

Engineering Structures

journal homepage: www.elsevier.com/locate/engstruct

Optimal seismic retrofitting of existing buildings considering environmental impact

Nicholas Clemett *, Wilson Wladimir Carofilis Gallo, Gerard J. O'Reilly, Giammaria Gabbianelli, Ricardo Monteiro

University School for Advanced Studies IUSS, Pavia, Italy

ARTICLE INFO

Keywords:
Environmental impacts
Optimal retrofit
Multi-criteria decision analysis
Life cycle assessment

ABSTRACT

The seismic performance of existing buildings can be improved significantly through the installation of various retrofit technologies. Decision support systems can be used for the selection of an optimal retrofit alternative when several important decision variables (DVs) need to be considered. Typically, the decision-making process considers a range of economic, social and technical aspects that are of interest to decision-makers; however, less or no consideration is given to the environmental impact (EI) of the retrofit alternatives. This study investigates how including the EI of possible retrofit alternatives as an additional DV in a multi-criteria decision making (MCDM) process can affect the choice of the optimal retrofitting scheme for a reinforced concrete school building in Italy. An assessment methodology for determining the life cycle EIs for the case-study structure, based on environmentally extended input-output life cycle analysis, is described. Then, a set of five retrofit alternatives is developed using response estimates from non-linear static analyses and their performance is assessed using non-linear time-history analysis and the PEER-PBEE framework. Several decision assessments are conducted, using the MCDM framework, each considering a subset of 13 possible DVs, including EI, to select an optimal retrofitting alternative. The results of the MCDM assessment and their implications are discussed in detail. The main conclusions were: (1) in some instances the expected annual EI may be a suitable proxy for the total life cycle EI when used in the MCDM framework; (2) the use of aggregated performance metrics such as the Life Cycle Performance Metric should be carefully considered when the MCDM procedure is used for the decision analysis, and; (3) the most significant factor affecting whether or not the inclusion of EI will affect the choice of optimal alternative is the weights of the DVs assigned by the decision-maker.

1. Introduction

A significant portion of the Italian building stock consists of structures built in the years following the second world war but before the introduction of the first seismic design codes in the 1970s. As a result, many of these structures have not been designed or detailed to withstand seismic demands and pose a significant risk in terms of economic losses and casualties [1]. Seismic performance can be improved either by demolishing and replacing the most at-risk structures with new code-compliant ones or retrofitting them to improve their seismic performance. Demolition and replacement of existing buildings is not generally considered an acceptable solution given the high capital costs associated with new construction, as well as the extended interruption caused to occupying residents and businesses [2]. In addition to these economic factors, there are significant environmental concerns associated with demolition and reconstruction. The building sector contributes approximately 40% of the total energy use and greenhouse gas (GHG) emissions in the EU [3] and, although the majority of this is associated with the operation of these buildings, a non-negligible portion can be attributed to their demolition and construction. Construction and demolition waste is also the most significant waste stream in the EU, contributing over 800 million tonnes of waste per year, or approximately 25% to 30% of the EU's total waste [4]. Considering that the economic and environmental costs of retrofitting are lower than wholesale demolition and replacement it is easy to see why this is the preferred option when deciding how to improve existing buildings' seismic performance.

When developing structural retrofit solutions, three main strategies can be used to improve a structure's seismic performance: (1) local strengthening of individual elements; (2) the introduction of additional

* Corresponding author.
E-mail address: nicholas.clemett@iusspavia.it (N. Clemett).

https://doi.org/10.1016/j.engstruct.2021.113391
Received 8 March 2021; Received in revised form 6 September 2021; Accepted 14 October 2021
Available online 13 November 2021

lateral load resisting elements, and; (3) the reduction of the demands on the structure via supplemental devices [5]. There are numerous ways in which specific retrofit schemes can encompass one or more of these strategies. Take, for example, the case of a typical reinforced concrete (RC) frame structure with unreinforced masonry (URM) infills designed prior to the introduction of seismic design codes. These structures may suffer premature shear failure of the joints due to inadequate detailing or shear failure of columns due to their interaction with the URM infill panels. Local intervention schemes aimed at strengthening the weak joints could include the application of fibre-reinforced polymer (FRP) sheets [6–8] or joint enlargement through the application of concrete jackets [8–10] or post-tensioned steel angles [11]. FRP and concrete jacketing can also be applied to the columns to increase their shear strength, flexural strength or ductility [8]. Alternatively, new or additional lateral load resisting elements can be added to create an alternative load path, thus reducing the demands on the existing elements. It is common for existing frames to be retrofitted with RC shear walls [2,8,12] or steel braces [8,13,14]. Moreover, the reduction of seismic demands can be achieved through the use of supplemental damping systems, such as viscous dampers [15,16] or base isolation [2,17,18].

There has been significant focus in recent years on developing methodologies that aim to determine an optimal retrofit configuration for a specific building. In the literature, optimal retrofitting can be achieved in one of two ways: (1) selection of an optimal solution from a predefined set of alternatives or; (2) optimisation of a specific retrofitting design using advanced computational methods, such as evolutionary algorithms. Studies using advanced optimisation algorithms [19–22] have shown that very cost-effective solutions can be achieved for different retrofitting schemes. Typically, these studies utilised non-linear static procedures for the seismic assessment of the design alternatives and the optimisation is performed on the basis of the total installation cost of the retrofit scheme, although future effort could be directed towards expanding optimisation criteria to include additional variables. On the other hand, methods for the selection of an optimal retrofit solution from a set of pre-defined alternatives proposed in the literature include: seismic resilience-based assessments [23–25]; index-based methods [26]; cost-benefit analyses [27–29]; and Multi-Criteria Decision Making (MCDM) [30,31], amongst others. Each of these methodologies uses structural response characteristics, economic variables, or a combination of both, to determine the optimal retrofit alternative from a set of candidates. The MCDM method is a more comprehensive decision support framework, which can accommodate a broad range of decision variables encompassing economic considerations, structural response, social aspects and environmental impacts (EIs) to name a few. Recently, Carofilis et al. [32] undertook a detailed assessment of a number of these methodologies within the context of selecting an optimal structural retrofit scheme for an existing RC school building in Italy. Their investigation revealed that the ranking of alternatives derived from selection methodologies with a strong focus on structural response often contradicted the rankings obtained from methods that relied on economic variables. When additional factors associated with social, aesthetic or practical aspects of the interventions were considered, yet another ranking of the alternatives was observed using the MCDM framework. In light of this, Carofilis et al. [32] concluded that simple decision-making tools, such as cost-benefit analysis or index-based methods, do not appear to be comprehensive enough when a wide variety of decision variables need to be considered.

In recent years, the assessment of a building's environmental impact has become increasingly important as building owners and property developers work to comply with new environmental regulations [3] or obtain green building accreditations from third-party organisations [33,34]. It would therefore be beneficial to consider the EIs associated with alternative designs when selecting an optimal structural retrofit solution. Several studies have considered or proposed metrics for evaluating different structural designs or retrofit alternatives in terms of their EI. The most common method in the literature is a direct comparison of the total EI for each design, usually normalised per unit of floor area [35–37]. Direct comparison of aggregated EI metrics, such as the BEES score, which is a weighted average of all of the EIs produced by a product [38], has also been utilised in several studies [39,40]. An environmental cost-benefit analysis has also been proposed in other studies [41–43]. Recently, Caruso et al. [44] proposed a comprehensive Life Cycle Performance Metric (LCPM) for evaluating the EIs of structural and energy efficiency retrofitting alternatives. This LCPM calculates the total economic costs or EIs over the life cycle of a building and expresses them in terms of €/m^2/yr. or $kgCO_2e/m^2$/yr. The LCPM is a flexible parameter that can incorporate costs or EIs from an array of sources including, but not limited to, retrofit installation, repair of seismic damage, maintenance, and energy use.

Despite the ability of these metrics to effectively communicate the EIs associated with different retrofit alternatives, to the authors' knowledge, they have yet to be included as part of a comprehensive MCDM methodology to select an optimal retrofit solution for an existing building. With this and all of the above in mind, the aim of the present study is to build on the work of previous studies, such as the one by Carofilis et al. [32], and investigate how the inclusion of EIs in the decision-making process can influence the selection of an optimal retrofit solution for existing buildings. A detailed seismic performance and EI assessment will be performed for an existing case-study building, which is characterised by poor seismic structural performance, located in a high seismicity region in central Italy. A selection of five retrofit alternatives will be developed for the structure in accordance with the requirements of the national design codes [45] and the recently developed Italian seismic risk classification guidelines [46]. Following the detailed assessment of each of the retrofit alternatives, the selection of an optimal retrofit solution will be investigated using the MCDM framework and the impact of EIs on such a choice will be scrutinised.

2. Assessment and selection methodology

2.1. Seismic assessment

This study features two distinct phases of structural performance assessment. The first phase involves using a simplified non-linear static procedure to estimate the displacements at which the as-built and retrofitted structures attain different performance limit-states (performance points) stipulated by the Italian building code (NTC) [45]. The N2 assessment method [47] was adopted for this study as it is one of several acceptable assessment methods outlined in the NTC [45]. As part of the initial seismic assessment of the as-built configuration, the N2 method can be used to identify critical structural weaknesses that limit the performance of the building and help guide the design of the various retrofit alternatives.

In the second phase of the analysis a detailed seismic performance and loss assessment is performed utilising non-linear time-history analyses (NLTHA) and the well established PEER-PBEE methodology [48]. The PEER Performance Assessment and Calculation Tool (PACT) is used to perform the required loss assessment calculations. A further description of the PEER-PBEE assessment framework and its implementation can be found in the FEMA P-58 series of reports [48–51] or the work by Günay and Mosalam [52].

2.2. Environmental impact estimation

The methodology used in this study to assess the EIs of the case-study building is based on the concept of Life Cycle Assessment (LCA), which is a common approach for assessing the cost and EI associated with the different phases of a structure's life. Typically LCAs consist of four steps: (1) definition of the scope of analysis and system identification; (2) compilation of the life cycle inventory (LCI); (3) impact assessment; and (4) interpretation of the results [53,54].

2.2.1. Stage 1: Scope definition

Step one focuses on determining the boundaries of the system for which the LCA is to be conducted. Fig. 1 shows the life cycle phases and a selection of processes that can be considered in the LCA of a typical building.

As the aim of the present study is to include consideration of EIs in the selection of optimal structural retrofit schemes, the scope of the impact assessments conducted in this work (Fig. 2) will focus on the estimation of both the pre-use and recurring embodied EIs, with no attention given to operational EIs (Fig. 1): the implicit assumption here is that the as-built and retrofitted structures all have the same operational EIs. This is deemed a reasonable assumption given that the structural retrofit interventions exclusively target improved seismic performance and not energy efficiency. The chosen system boundary encompasses all five of the major life-cycle stages shown in Fig. 2 - extraction, manufacture, construction, use and end-of-life - and is considered to be a cradle-to-grave assessment. As Fig. 2 illustrates, the effects of transportation and labour have not been explicitly considered in the EI assessment. Labour is not typically considered in the building LCA as human labour does not contribute directly to any EIs [55]. Transportation, on the other hand, has a clear impact on the environment, however, these impacts are difficult to quantify unless detailed information is obtained relating to local conditions (e.g. distance from material sources and waste dumps). Excluding the transportation impacts is expected to have a minimal effect on the overall results and conclusions drawn, given that all of the retrofitted structures are likely to be affected equally. Four different system boundaries are used to estimate the EIs in different parts of the study and these are illustrated in Figure F4. The red boundary represents the cradle-to-gate EIs associated with repairing earthquake-induced damage. In this system, the construction EIs have been neglected as the LCI database used only provides information for a cradle-to-gate assessment. More details regarding the chosen LCI database are provided in Section 2.2.2. End-of-life effects were also not considered as they are accounted for separately in the building replacement system (blue boundary). The EIs of building replacement systems are also calculated from the LCI database, however, they can be calculated by applying the replacement cost to the "school and vocational buildings" industrial sector, which includes construction costs. This system is the only system that considers the impacts associated with the labour and transportation required to reconstruct the structure because these are implicitly included in the EI per unit cost value of the sector. In this case, the end-of-life EIs can be accounted for by amplifying the pre-use embodied impacts by a fixed amount, as will be discussed in Section 4.4. The green line represents the boundary of the system assumed when calculating the EIs for the installation of the retrofit alternatives. Here, the same assumptions were made as for the repair system, except that an allowance has been made for the EIs resulting from the disposal of construction waste. This was possible because the design of the retrofit alternatives made it easy to provide an estimate for the expected volume of waste. Finally, the bold black line indicates the complete system boundary that has been used to estimate the total life-cycle environmental impacts (LCEI) for the structure and it is the result of the union of the systems previously described plus the maintenance EIs.

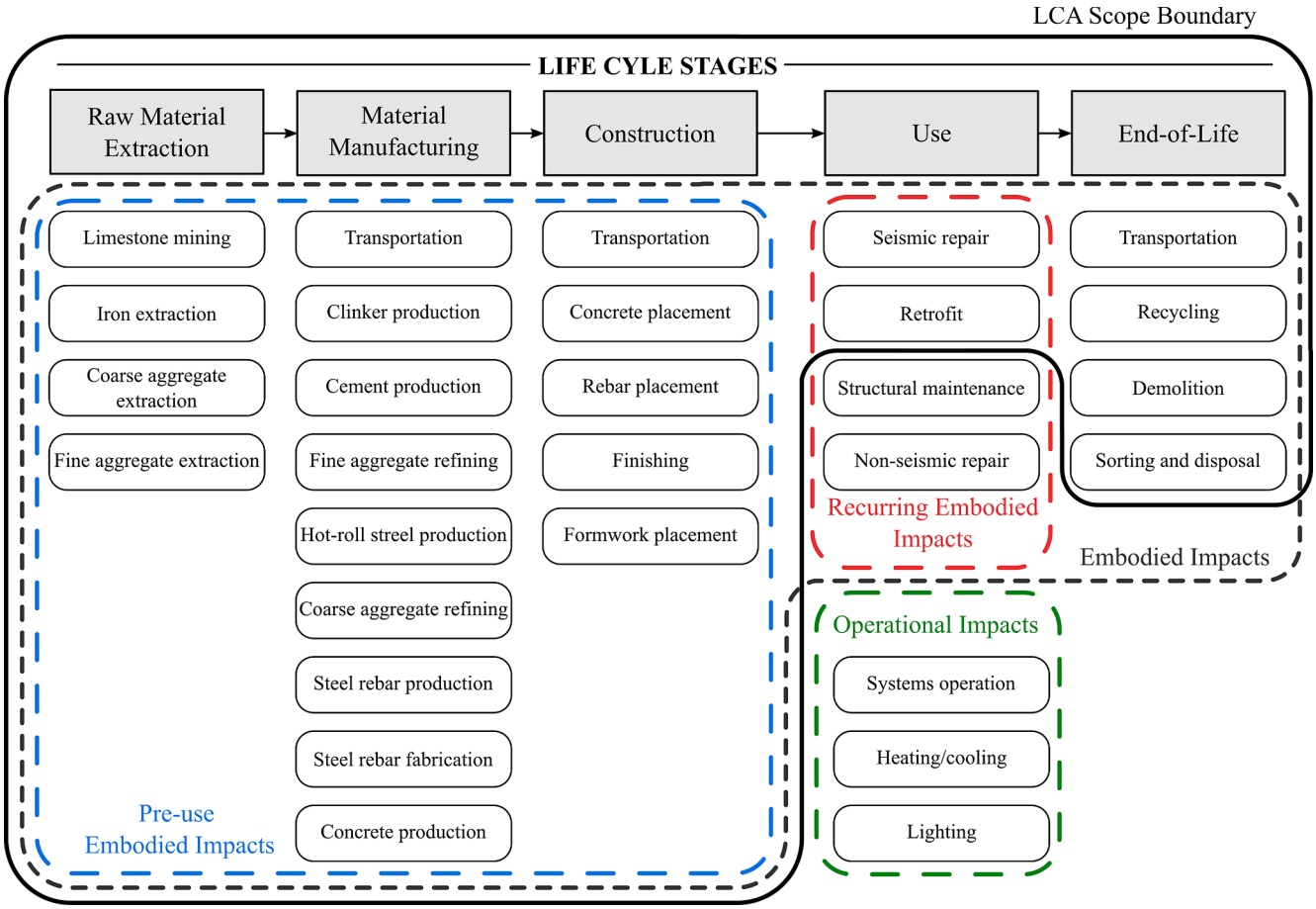

Fig. 1. Schematic of the typical life-cycle phases and a selection of possible processes that could be considered in an LCA. The colour lines indicate the boundaries of different categories of EIs.
Adapted from [36]

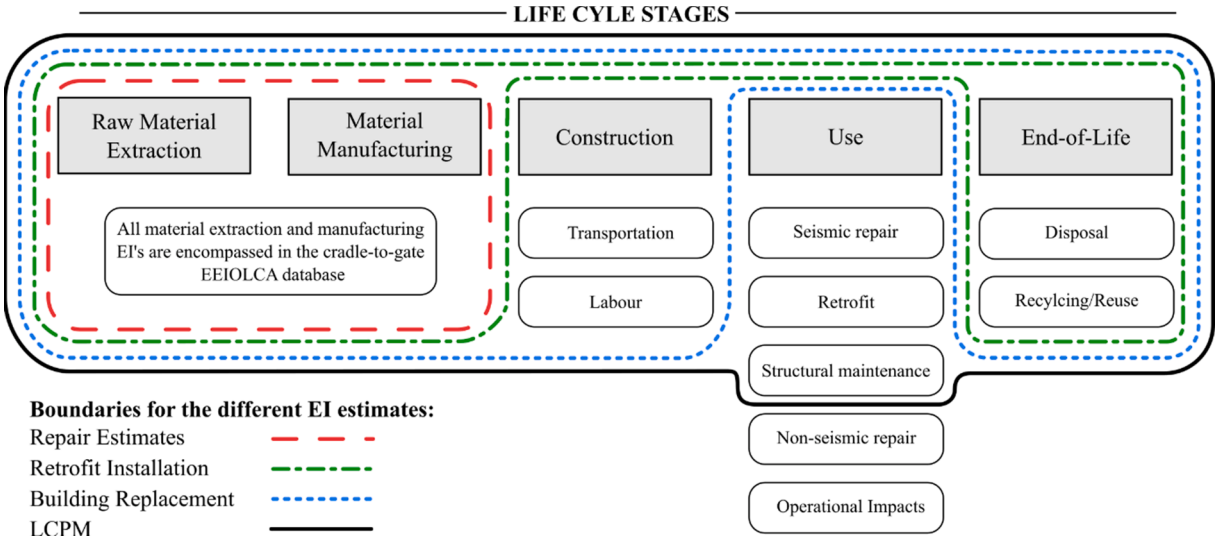

Fig. 2. Scopes of the different EI assessments conducted as part of this study.

2.2.2. Stage 2: Life cycle inventory

Step two of the LCA process is the compilation of the life cycle inventory (LCI), which is a collection of all of the processes, industries and sources of EI that fall within the system boundary specified in step one. The ISO guidelines do not standardise the methods that are used to develop life cycle inventories. In previous studies examining the EI of buildings subject to seismic damage Process-based LCA (PLCA) [35,37,39,40,56–60], Environmentally Extended Input Output LCA (EEIOLCA) [36,44,61,62] and carbon factor [41,42,63–65] LCI have been employed.

In the present study an EEIOLCA inventory was selected for use, specifically the USEEIO life cycle inventory [66]. This proves to be an attractive choice for several reasons. Firstly, the data from the USEEIO database has recently been integrated into PACT (version 3.1.2) [49], which, as highlighted in Section 2.1, is the primary performance assessment tool used in this study. Secondly, using an EEIOLCA inventory makes it relatively straightforward to determine the EIs associated with the repair of components that are not already included in the PACT fragility database, as they can be estimated using repair cost estimates obtained from literature, e.g. [67,68]. The functional unit of the USEEIO inventory is EIs/$US (2013). When calculating the impacts for a year other than 2013, the effects of inflation should be considered. Additional information regarding the comparison between EEIOLCA inventories and PLCA inventories and associated sources of error can be found in references [55,61,69,70].

2.2.3. Stage 3: Impact assessment

In this phase the resources consumed and the emission and waste flows generated by the processes and industrial sectors identified in step two are converted into EIs, using a library of EI factors that simplify a large catalogue of emissions into several, more communicable, performance metrics [54,71]. This study has chosen to use Climate Change Potential (CCP), measured in equivalent kilograms of carbon dioxide ($kgCO_2e$) as the sole metric for assessing the EI of the case-study building because it has been shown to be a good proxy for a range of different EIs [55]. The impact assessment for the as-built structure, the installation of the retrofit schemes and the repair of seismic damage can be assessed by directly applying the disaggregated sector costs for each life-cycle phase to the values from the USEEIO matrix. In these calculations, a 2020–2013 deflation factor of 0.91 was considered [72]. The flowchart in Fig. 3 illustrates the impact assessment procedure.

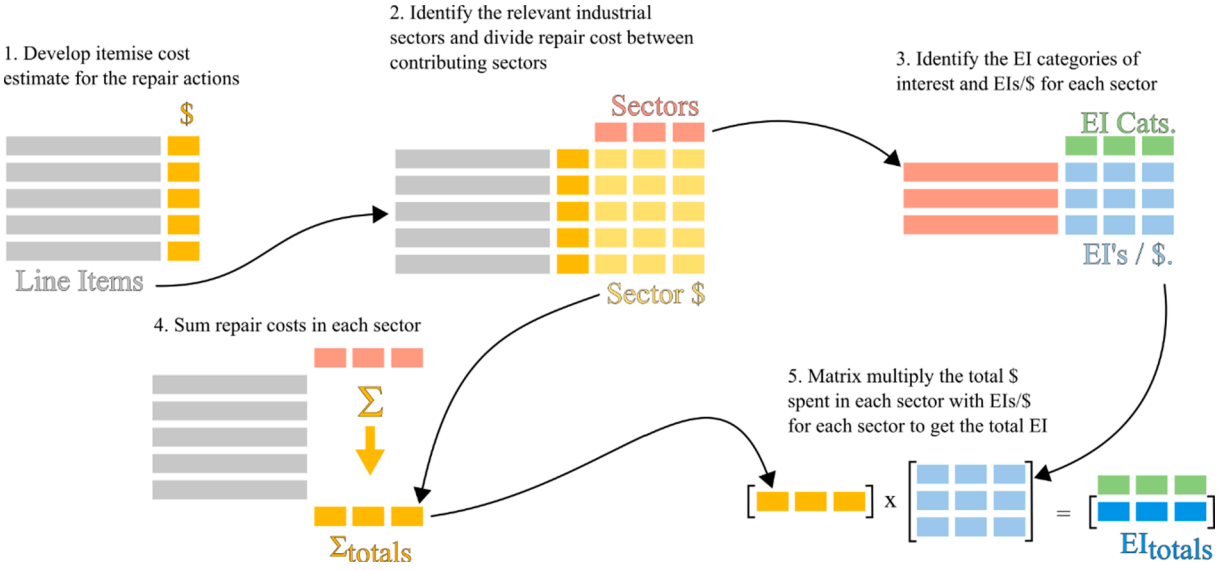

Fig. 3. EEIOLCA impact assessment procedure adapted from Huang and Simonen [61].

2.2.4. Stage 4: Interpretation of results and sources of uncertainty

The final step in an LCA is the interpretation of the results. This typically includes the identification of the process or materials that contribute most significantly to the total EI. The results should also be presented in terms of a useful performance metric along with a discussion of the data quality and uncertainties in the calculation. This step is key in facilitating comparisons between different products or, as in the present study, different building retrofit alternatives. The results of the impact assessments will generally be presented in terms of $kgCO_2e$/building for the pre-use embodied impacts or $kgCO_2e$/yr for recurring embodied impacts, enabling a good comparison between the as-built structure and the different retrofit alternatives. Some of the limitations and potential sources of uncertainty relevant to EEIOLCA inventories are highlighted by Säynäjoki et al. [69] and Majeau-Bettez et al. [70], however there are other sources of uncertainty that are introduced in this particular study. Firstly, the USEEIO inventory has been developed using US economic data meaning that the EIs derived from its use are applicable only within the United States. The application of this inventory to case studies outside of the US will likely increase the error of the impact estimate unless it can be demonstrated that the economy of interest has the same structure as the US economy. In this study, the use of the USEEIO inventory for a case-study building in Italy is justified by the fact that the assessments performed are for comparative purposes and any error resulting from the use of a US inventory will likely have an equal effect on all of the retrofitted structures. Secondly, the USEEIO database does not consider any sort of uncertainty in the EI estimates for each sector, however, uncertainty in these values is accounted for in the PACT software by assuming that the uncertainty of the EIs (β_{EI}) is related to the uncertainty of the cost estimate (β_C), as given by Equation (1):

$$\beta_{EI} = \sqrt{\beta_c + 0.25^2} \tag{1}$$

2.3. Optimal retrofit selection

Extending on the work of Carofilis et al. [32,73], the MCDM framework has been chosen to aid in the selection of the optimal retrofit scheme for the case-study structure and its application has been described extensively by Caterino et al. [30]. This study considers a broad range of decision variables (DVs), encompassing the social, environmental and economic aspects of each retrofit alternative and a complete list can be found in Section 7.1. These criteria have also been adopted in previous studies by Caterino et al. [30] and Gentile and Galasso [31], with the exception of the EI variables, and the rationale for the selection of these variables can be found in those papers. For what concerns the EI DVs, the EI of installation, C_9, was selected because it is analogous to the cost of installation and represents an initial capital investment associated with the retrofit scheme. Conversely, the expected annual EI (EAEI), C_{10}, represents an ongoing environmental cost associated with the retrofit alternatives and is impacted by the seismic performance (i.e. the effectiveness) of the retrofit alternatives. Economic and environmental LCPMs [44] have also been included to investigate what effect aggregating all life-cycle costs and EI factors into only two DVs will have on the selection of the optimal alternative.

The weight vector values used in this study have been derived from the data collected in the survey conducted by Carofilis et al. [73], which received responses from researchers and engineers practising in the field of structural earthquake engineering and retrofit in Italy. The specific values of the weight vectors and decision matrices used in each of the MCDM analyses performed as part of this study are reported in Section 7.1. In addition to conducting the survey, Carofilis et al. [73] also investigated the effects of considering uncertainty in the MCDM framework. One of their key findings was that, when the values in the weight vector are relatively uniform, the inclusion of uncertainty in the weight vector and the decision matrix has little effect on the overall ranking of the alternatives. With this in mind, the present study will use the deterministic method described in Carofilis et al. [73] to select the optimal retrofit alternative.

3. Case-study building

3.1. Characteristics and properties of the case-study structure

The building chosen as the case study for this research is an RC moment-resisting frame (MRF) school building with URM infills located in Isola del Gran Sasso d'Italia, Abruzzo, Italy [74]. The school consists of two above-ground storeys and a small partial basement at the east end. The first and second floors each have an area of approximately 630 m^2 and interstorey heights of 3.75 m and 4.25 m, respectively. The structural system consists of two-way RC MRFs in the longitudinal (X) and transverse (Y) directions. URM infills and partitions are present throughout the building and large penetrations in the exterior infills allow for the presence of windows. As this structure was built sometime between the 1960s-1970s, it is an example of the typical Italian construction prior to the introduction of modern seismic design codes [74]. A more detailed description of the building, along with architectural plans and elevations, can be found in Prota et al. [74].

3.2. Numerical modelling

For the case-study school building, a numerical model was developed using the OpenSees software framework [75]. A three-dimensional representation of the numerical model is presented in Fig. 4. The model consists of flexural elements (i.e. beams and columns), beam-column joints (BCJs), a stair-case, and masonry infills. The typical frame elements (beams, columns and BCJs) were modelled following the suggestions presented by O'Reilly and Sullivan [76] for simulating the structural behaviour of older Italian RC frames. The staircases were modelled using simple elastic frame elements, with one element representing each stair unit. The concrete and steel material properties were obtained from Prota et al. [74]. More information on the modelling of the RC frame elements for this case-study structure can be found in the studies of Carofilis et al. [32,73].

The effects of the exterior masonry infills on the response of the structure was modelled by incorporating a system of equivalent diagonal struts that represent the behaviour of the infills [77]. The case-study structure features four different infill configurations, which, along with the corresponding equivalent strut configurations, are presented in Fig. 5. All four of the equivalent strut configurations have been modelled following the recommendations of Sassun et al. [67], assuming that the hollow masonry blocks have the same geometry and material properties as the T3 typology used by Hak et al. [78]. For the partial height infills (Fig. 5c and d), the strut parameters were determined assuming the actual height of the masonry infill, below the window penetrations. In these cases, no additional stiffness or strength reductions due to window penetration were considered. In the case of the partial width infill (Fig. 5b) the stiffness and strength reduction factors proposed by Decanini et al. [79] were used to modify the properties of the infill struts to account for the window and door penetrations. The strut models used in these analyses are only capable of modelling the in-plane behaviour of the infills. To simplify the analysis and the post-processing, no consideration has been given to the out-of-plane (OOP) behaviour of the infills.

It is acknowledged that, by using this simple single strut model, the collapse performance of the structure could be overestimated and the losses underestimated, given that shear failure of the columns is not being accurately modelled. In this study, this was not considered to be a significant liability because each of the retrofitting solutions specifically addresses the negative impacts of column-infill interaction, as will be detailed in Section 5.4.

In addition to the modelling of the specific structural elements, the *laterizio* floor system was assumed to be rigid, which is typical of other similar studies [44,80,81]. The second-order geometric effects have been modelled using the P-Δ formulation. The base nodes of the

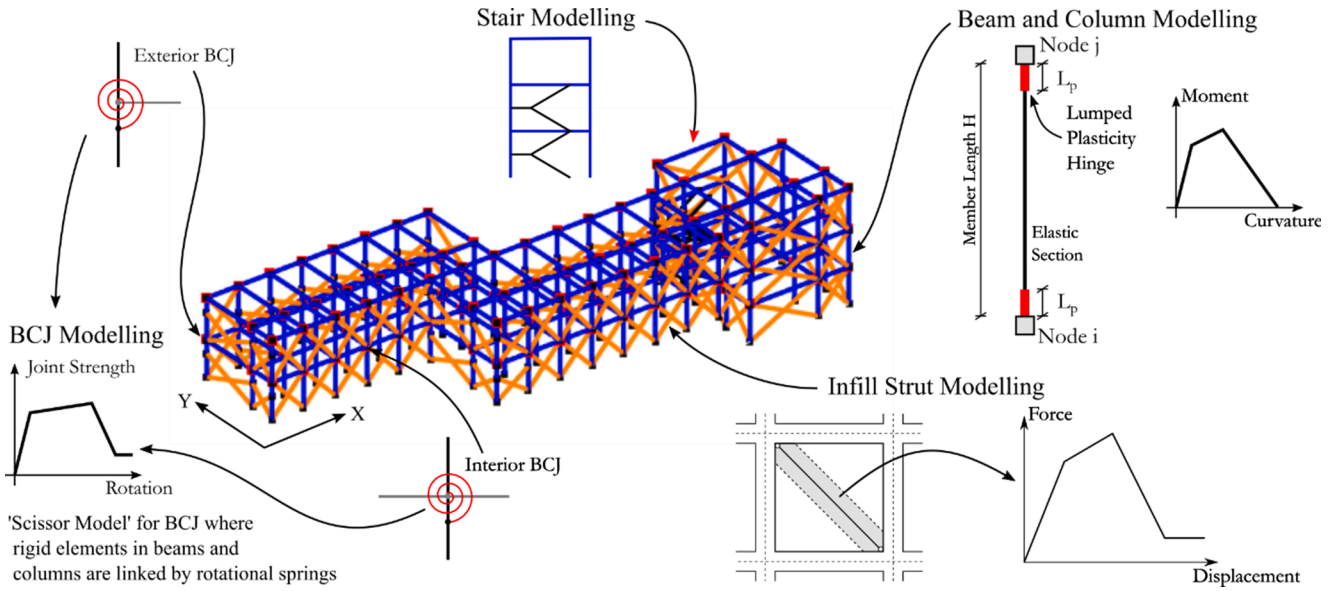

Fig. 4. 3D representation of the numerical model developed in OpenSees. Blue members are force-beam-column elements, black members are elastic elements and orange members are truss elements. Qualitative backbone curves for the non-linear elements are also shown. Adapted from Carofilis et al. [32].

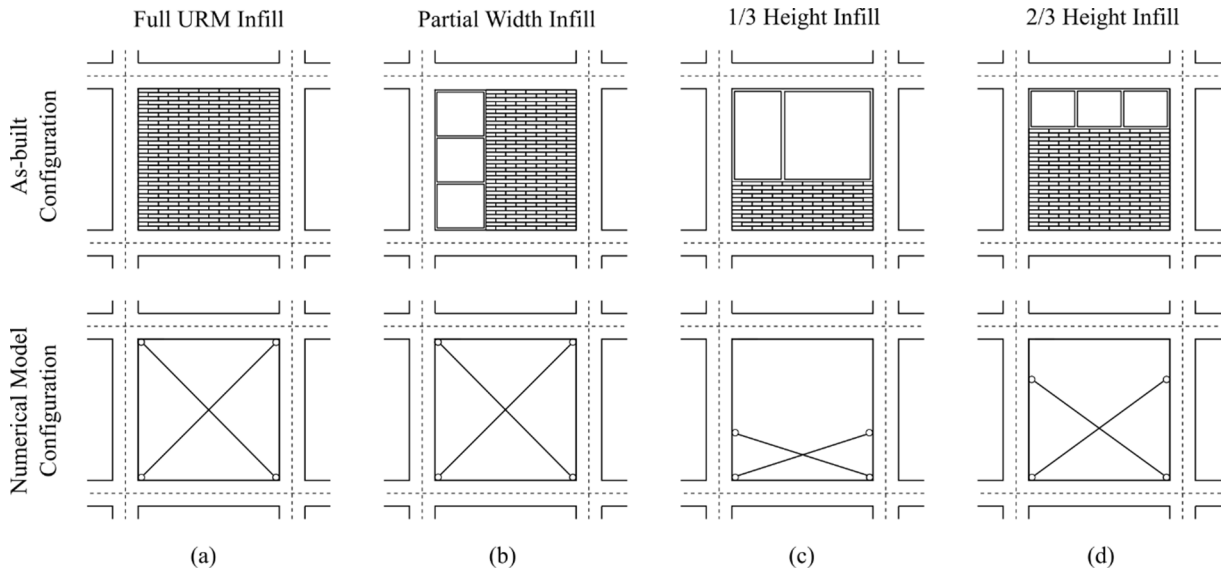

Fig. 5. Different infill configurations present in the case-study structure and the equivalent strut geometry adopted in the numerical model.

numerical model were considered to be fully fixed and any effects resulting from soil-structure interaction were neglected. Finally, 5% tangent stiffness proportional Rayleigh damping was adopted at the frequencies of the first and third fundamental modes of vibration.

3.3. Preliminary assessment of as-built structure

Before the design of the alternative retrofit schemes, the performance of the as-built structure was assessed. The NTC [45] defines four limit states: Operational limit state (SLO); Damage limitation limit state (SLD); Life safety limit state (SLV), and; Collapse prevention limit state (SLC). For a school building, which is characterised by the NTC [45] as a class III building, the specified design life is 75 years and the ground motion return periods corresponding to each limit state are: SLO, 45 years; SLD, 75 years; SLV, 712 years, and; SLC, 1463 years.

The performance of a structure is generally quantified using either global displacements, local deformations, strength capacity checks or a combination of all three. The NTC [45] requires several demand-capacity/limit checks to be performed at each limit state, which are presented in Table 1. In addition to the interstorey drift, flexural hinge rotation and beam/column shear resistance checks, using the capacity models provided by the NTC [45], verifications of the rotation capacity of the BCJ springs and axial strain of the infill struts were performed to provide a more comprehensive assessment of the building's performance. These are summarised in Table 1.

The interstorey drift limits defined in the NTC [45] for class III structures with fragile non-structural components (such as URM infills) are 0.33% at SLO and 0.5% at SLD. The limits on the maximum rotation/curvature of the beam/column flexural hinges and the moment capacity of the BCJs were calculated following the requirements and the equations from Section C8.7.2.3 of the supplement to the NTC [45] for the assessment of existing structures. The shear failure of the beams and columns was checked using the expressions provided by the NTC [45] which define the capacity based on the well-known truss analogy, with

Table 1
The structural verifications stipulated by NTC [45] for each limit state are indicated by black dots. Additional checks carried out are indicated by the squares. The verifications highlighted in grey indicate that the as-built structure failed this verification based on the results of the simplified seismic assessment.

		SLO	SLD	SLV	SLC
Global Displacement	Interstorey drift	●	●		
Local Deformation	BCJ rotation				■
	Beam hinge curvature		●	●	●
	Column hinge curvature		●	●	●
	Infill strut axial strain	■	■	■	■
Strength Demand-Resistance	Beam shear			●	
	Column shear			●	
	BCJ Moment			●	

the strut inclination and concrete and steel resistances being determined based on criteria provided in the code. The maximum acceptable BCJ rotation was set at 0.02 rad, based on the recommendations of O'Reilly and Sullivan [76] who evaluated several past experimental tests on such sub-assemblies. The infill strut strain limits were adopted based on the recommendations of Sassun et al. [67], which were also used in the definition of the modelling approach in order to be consistent throughout.

A displacement-controlled non-linear pushover analysis of the structure was performed using an inverted triangular load pattern and a control node located at the centre of mass on the top floor. For each of the limit states, the results from the pushover analysis were used in conjunction with the N2 method, outlined in Section 2, to estimate the performance of the structure. It is worth noting here that the N2 method was not specifically developed for use with irregular URM-infill structures and it has been shown that there may be some inaccuracy in the results obtained when used in this context [82]. However, for this study, in which the N2 method has been used for just an initial seismic assessment and rapid design of possible retrofit alternatives, these inaccuracies are not expected to be of notable consequence. The detailed seismic assessment, which employs a more detailed NLTHA, has been used to determine the values of the parameters used in the final decision assessment.

The performance points obtained from the N2 assessment were compared with the displacements at which the various structural elements reached their deformation or strength limits corresponding to each applicable limit state. The pushover curves summarising these analyses are presented in Fig. 6a. The critical structural weaknesses at SLV are the moment capacity of the BCJs and the shear failure of the short columns located adjacent to the partial height URM infills. These elements limit the performance of the structure to such an extent that failure occurs before the structure reaches the expected displacement demand induced by an SLO intensity ground motion. At SLO intensities, the axial strain of the infill struts also exceeds the SLO limits proposed by Sassun et al. [67].

Fig. 6b presents the drift profiles at the structure's centre of mass in both the X and Y directions at each of the four limit state performance points. The corresponding drift limits are shown for comparison. The maximum drifts at SLO and SLD intensities are estimated to be 0.19% and 0.21% respectively, which is well below the code specified limits. It

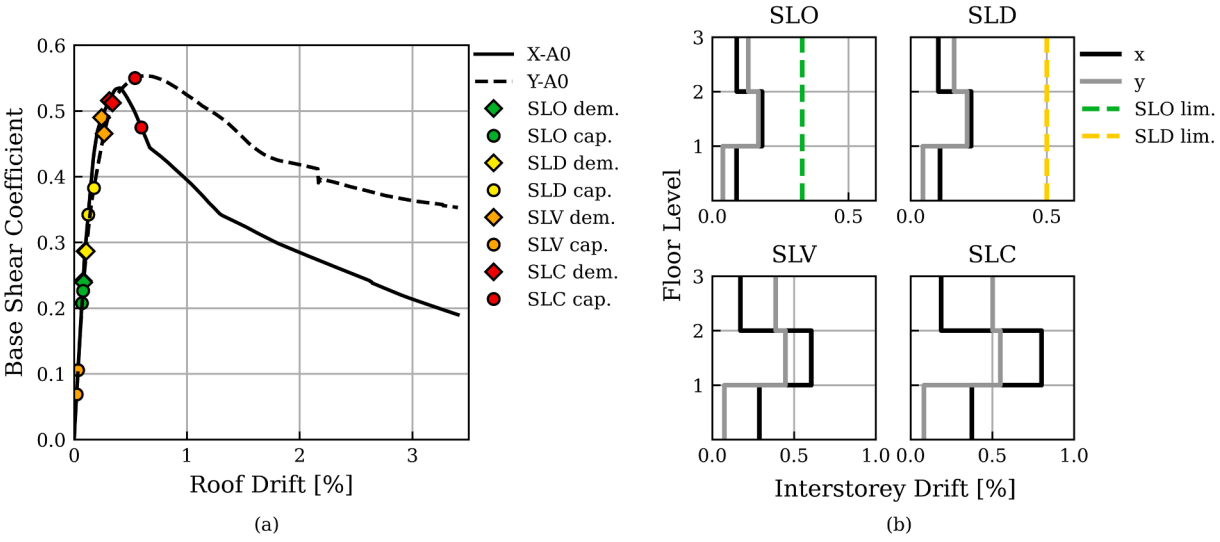

Fig. 6. (a) Pushover curves showing the N2 performance points (diamonds) and the capacity (circles) at each limit state for the as-built case-study structure. (b) Drift profiles for each of the four limit states in the X and Y directions and the code specified drift limits.

should be noted, however, that it appears that the structure may be susceptible to the formation of a soft-storey at level two for higher intensity ground motions. This can be attributed to the fact that the strength and stiffness of levels two and three are similar, but the higher shear force at level two causes the corresponding infills to fail first. This results in reduced strength and stiffness of level two relative to level three, leading to a concentration of drift.

The results of modal analysis of the as-built structure (A0) are presented in Table 2 along with the results of the other retrofitting alternatives (A1 to A5) discussed in subsequent sections.

3.4. Proposed retrofit alternatives

3.4.1. General description

Calvi [2] notes that it is often counter-productive to invest significant amounts of resources to strengthen existing structures to meet the code requirements for new structures. Retrofitting a structure to increase its seismic performance, even if it does not meet the all of the code-define capacity requirements for new buildings still represents a significant improvement over the original as-built configuration and would be in line with the goals of recent risk-reduction programmes, such as the Italian Sismabonus scheme [46]. This simple principle has been used in this study to guide the design of the five retrofit alternatives being proposed. Where it is deemed practical, the design of the retrofit schemes attempts to meet the code-defined limit state requirements; however, where this cannot be achieved (e.g. due to excessive cost or material requirements) the maximum improvement that can be realistically achieved is accepted even if the performance is technically less than required by the NTC [45]. The following paragraphs, Table 3, and Fig. 7 provide a summary of the five retrofit alternatives considered in this study.

A significant retrofit intervention that has been investigated in other studies (e.g. [83]) and applies to all five of the retrofit alternatives is the inclusion of a seismic gap of 50 mm between masonry infills and columns. This corresponds to a storey drift of approximately 1.3% and is over two times larger than the maximum drift of A0 at SLC. The inclusion of this gap significantly reduces the risk of column shear failure resulting from the column-infill interaction, but it will result in a more flexible structure, leading to increased displacements. These displacements can be controlled by the new retrofit schemes in a way that does not risk shear failure in the columns. It is also noted that the introduction of the seismic gap does significantly increase the risk of OOP failure of infills although this can be reduced by installing OOP restraints to the sides of the infill and the application of a fibre reinforced plaster to increase the tension capacity of the infill [84]. The reduction in thermal performance could also be remediated by filling the seismic gap with a compressible insulation material or a compressible grout with very low elastic modulus, although these considerations are outside the scope of this study.

Table 2
The first four modal periods, geometric mean (T_{GM}) and period range of the six models used in this study. The labels X_i, Y_i and Tr_i in parentheses indicate the i^{th} mode in the X-, Y-, and Torsional directions, respectively. The bold values are used to calculate the geometric mean used in the record selection.

	Mode 1	Mode 2	Mode 3	Mode 4	T_{GM}	$0.2T_{GM}$ – $1.5T_{GM}$
A0	0.311 (Tr_1)	**0.266 (X_1)**	**0.235 (Y_1)**	0.127 (Y_2)	0.250	0.050–0.375
A1	**0.603 (X_1)**	0.492 (Tr_1)	**0.367 (Y_1)**	0.234 (Y_2)	0.470	0.094–0.705
A2	**0.408 (X_1)**	**0.367 (Y_1)**	0.288 (Tr_1)	0.190 (X_2)	0.387	0.077–0.581
A3	**0.396 (X_1)**	**0.352 (Y_1)**	0.269 (Tr_1)	0.182 (Y_2)	0.373	0.075–0.560
A4	**0.750 (X_1)**	0.521 (Tr_1)	**0.348 (Y_1)**	0.297 (Tr_2)	0.511	0.102–0.767
A5	**0.339 (X_1)**	**0.190 (Y_1)**	0.077 (Y_2)	0.056 (X_2)	0.254	0.051–0.381

Table 3
Summary of the five retrofit alternatives considered in this study, the primary intervention techniques used, and their intended effect.

Alternative	Interventions	Effect
A1	CFRP strips to BCJ	Increases joint shear resistance
	CFRP bars to columns	Increases column stiffness and flexural capacity
	CFRP wrap of columns and beams	Increases shear resistance of elements and confinement
A2	Steel X-Braces around exterior	Reduces force and displacement demand on MRF
A3	CFRP as for A1	–
	Braces as for A2	–
A4	CFRP as for A1	–
	Viscous dampers	Reduces displacement and acceleration demands
A5	RC Shear walls	Reduces frame demands and regularises storey drifts
	CFRP wrapping as for A1	–
	Steel Joint Enlargement	Increases joint shear resistance

Following the separation of the infills, the first four retrofit alternatives (A1-A4) are the same as those presented in the recent work of Carofilis et al. [32,73] and a detailed description and discussion around the advantages of each alternative can be found in those publications. The final alternative, A5, designed for this study, uses a combination of RC shear walls, BCJ enlargement and CFRP wrapping to improve the seismic performance of the case-study building. The addition of RC shear walls provides a new system of lateral-load-resisting elements, thereby reducing demand on the existing frame. The walls are expected to regularise the interstorey drift and prevent the formation of a soft-storey at high levels of excitation. The length, strength and location of the walls were determined by attempting to move the centre of stiffness and centre of resistance of the structure to coincide with the mass and reduce the torsional response of the structure [85]. Six 1.5 m long shear walls have been provided in the X-direction, parallel to the longitudinal axis of the building, with two located along each of the north façade, south façade and central axis of the building. In the Y-direction (transverse axis), three 2.8 m long shear walls have been placed around the stairwell to reduce the torsional effects attributed to the relative position of the weaker columns. Two 1.5 m long shear walls were positioned on the west façade, with two more 2.0 m long walls located near the central axis of the building. All of the shear walls are 200 mm wide. The shear capacity of the BCJs was improved by installing a system of steel angles, plates and post-tensioned rods [11,86]. The capacity of these joints was verified using the strut-and-tie model developed by Shafaei and Nezami [86]. This post-tensioned steel system increases the effect of the size of the BCJ and provides additional confining pressure to the joint increasing the shear capacity. In several instances, the relocation of the beam and column hinges away from the BCJ caused an increase in the shear demand on the beams and columns. To ensure adequate shear capacity, CFRP jackets designed in accordance with Eurocode 8 [87] were applied to the affected elements.

3.4.2. Additional modelling considerations

First of all, and common to all five of the retrofit schemes, the infill-strut elements were removed from the models in response to the seismic separation of the infills and the frames. To accommodate this assumption, additional checks were carried out during the non-linear analyses to ensure that the estimated drifts did not exceed the 50 mm seismic gap provided.

As noted in the previous section, A1-A4 are the same as the retrofit schemes presented in [32,73]. A detailed description of the modelling considerations can be found in those publications and will not be repeated here. For A5, the RC walls have been modelled using fibre-

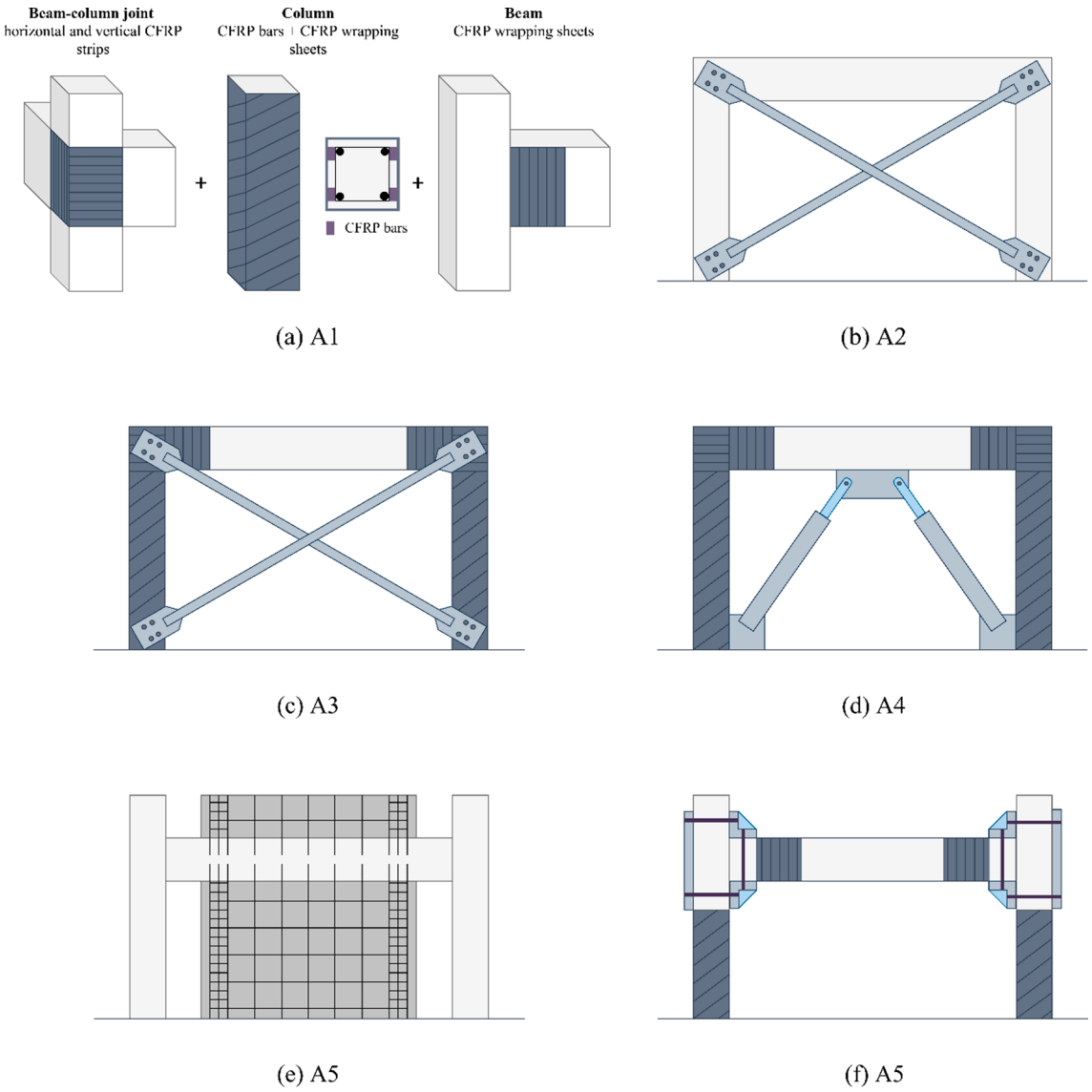

Fig. 7. Conceptual details of the five retrofit alternatives: (a) A1 – CFRP wrapping along with CFRP bars in columns and CFRP strips in joints; (b) A2 – steel bracing in specific bays; (c) A3 – combination of CFRP and steel bracing; (d) A4 – combination of CFRP and viscous dampers; (e) A5 – reinforced concrete shear walls installed in specific locations; (f) A5 – joint enlargement with a post-tensioned steel angle system.

section force-beam-column elements spanning between floors. Each element uses a four-point Gauss-Lobatto integration scheme to model the effects of distributed plasticity. The steel fibres are modelled using the Giuffré-Menegotto-Pinto material model with the recommended parameter values from Filippou et al. [88]. The unconfined cover concrete was modelled using the OpenSees concrete01 model with the key parameters taken from experimental tests [74] or being calculated using the simplified parabolic model described by Collins [89]. The confined concrete was defined using the same basic concrete model, except that the effect of the confining reinforcement was accounted for by increasing the ultimate compressive strength and ultimate strain of the concrete using the Mander model [90]. The yield strength of the steel was 550 MPa and the unconfined concrete strength was 38 MPa. The strain at maximum stress in the concrete is 0.002 and the ultimate concrete strain is 0.0035. In the locations of the walls, the existing beam elements were removed, assuming that the existing beams will be removed to allow the installation of the new walls. To account for the non-negligible mass associated with the installation of the shear walls, additional masses were added to the wall nodes at each storey. The total weight of the A5 structure was then taken as 7150 kN. The post-tensioned steel joint enlargement systems were modelled simply by extending the rigid end-blocks of the existing beam-column elements to account for the depth of the new steel angles (200 mm). The zero-length spring element representing the BCJ behaviour was assumed to be elastic for all retrofitted joints as the results of experimental testing of this system showed negligible cracking, even at extremely large displacements (10% drift) [11,86]. The stiffness of the retrofitted BCJ springs was determined from the capacity of the joint estimated from the strut-and-tie model and the cracking rotation of 0.0002 rad from the original BCJ model [76].

3.5. *Preliminary structural assessment of the retrofit alternatives*

The preliminary performance assessment of the retrofitted alternatives was conducted in much the same fashion as the as-built structure, denoted A0. A modal analysis was performed for each alternative, the results of which are presented in Table 2.

Following the modal analysis, non-linear pushover analyses were performed for each of the alternatives and the N2 procedure was used to determine the performance points of each structure. The implications of

this type of assessment for structures with additional supplemental damping, such as A4, are discussed by Carofilis et al. [32]. The results of the pushover analysis and N2 assessment are presented in Fig. 8. In addition to the limit state verifications highlighted in Table B, additional checks were also made on: the wall curvature at SLD, SLV and SLC; brace buckling at SLD, and; brace fracture at SLC. No verifications of the infills were performed for the retrofit alternatives because it has been assumed that the provision of a seismic gap greater than the maximum displacement observed at SLC will allow the infills to remain undamaged.

From Fig. 8, it is immediately clear that the initial stiffness and the lateral resistance of the retrofit alternatives are lower than A0, particularly in the X-direction. This is a direct result of the separation of the infills and the frame. The reduction in strength and stiffness is more pronounced in the X-direction than in the Y-direction because of the larger number of infills present in the longitudinal axis of the building. The key performance characteristics of A1-A4 at each limit state are described by Carofilis et al. [32]. For A5 the column deformation limit is exceeded at SLD; however, this occurs for only a small number of columns and the consequent implications are not significant. In the Y-direction, all of the member capacities are greater than the demands. At SLV and SLC, the improved performance of A5 is very evident with all capacities exceeding the expected demands.

The drift profiles of the retrofit alternatives for each of the four limit states are presented in Fig. 9. In general, the interstorey drifts are larger for the retrofitted alternatives, when compared to A0. This is a result of the separation of the URM infills from the MRF. The drifts are, in general, below the code specified limits, the notable exception being A5 at SLO. In this case, however, the expected drifts are not significantly larger than the limit and a more accurate drift performance will be assessed with detailed non-linear time-history analyses. The drift profiles also show that the formation of a soft-storey mechanism in the as-built configuration has been addressed.

4. Detailed seismic performance assessment

4.1. Characterisation of seismic hazard

The first step in the detailed seismic assessment procedure, as described in Section 2, is the characterisation of the seismic hazard at the location of the building of interest. This study adopted the same ground motion set selected as part of the studies of Carofilis et al. [32,73]. The record set is suitable for application to this study because the case-study building is located at the same site and the period ranges for models A0-A5 (Table 2) all fall within the range used to select the records (0.05–1.0s). Sets of 20 ground motion records, comprising two orthogonal horizontal components, were selected for ten return periods: 30, 45, 75, 100, 200, 475, 712, 975, 1463 and 2475 years.

4.2. Characterisation of structural response

Multiple-stripe analysis (MSA) [91] was conducted to characterise the response of the different structures using the records selected in the previous section. The key engineering demand parameters (EDPs) that were monitored and recorded for use in the loss assessment phase were the absolute peak floor acceleration (PFA), the peak storey drift (PSD) and the peak floor velocity (PFV). The medians of the maximum values observed for each EDP across all storeys at each intensity are presented in Fig. 10.

The most obvious point to note from these plots is the poor performance of A0, as anticipated based on the initial evaluation performed in Section 5. For intensities larger than those corresponding to a 200-year return period, the structure reached the collapse criteria, which are detailed in the following paragraphs, in all 20 records of the stripe. In general, the retrofitted structures performed significantly better, only recording failure in all records at a return period of 2475 years. Furthermore, the retrofitted alternatives tended to exhibit lower PFAs than A0 across the range of intensities, which was expected given the reduction in lateral stiffness of the structure. A significant improvement was noted in A1 and A4, in which the increased flexibility of the separated moment frame (A1) and the increased damping (A4) reduced the demands appreciably. The PSDs in the Y direction show a minor improvement when compared to A0. Conversely, in the X-direction higher drifts were observed by all of the alternatives when compared to A0, particularly A1 and A5, which tended to produce the largest drifts across the range of intensities. There is less variation between the PFV values of A0 and the retrofitted structures than the PFDs or the PFAs, however, the retrofitted structures do exhibit a minor reduction in PFVs.

Vectors of the maximum response of each EDP at each level of the structure were also recorded for each ground motion and will be used as

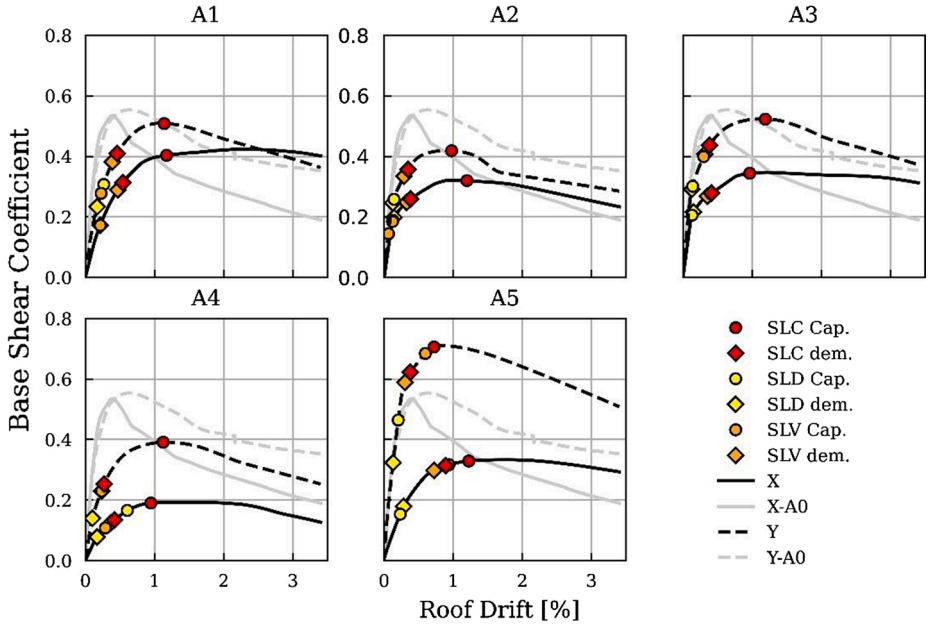

Fig. 8. Pushover curves, performance assessment and limit state capacities for the five retrofit alternatives at SLD, SLV and SLC.

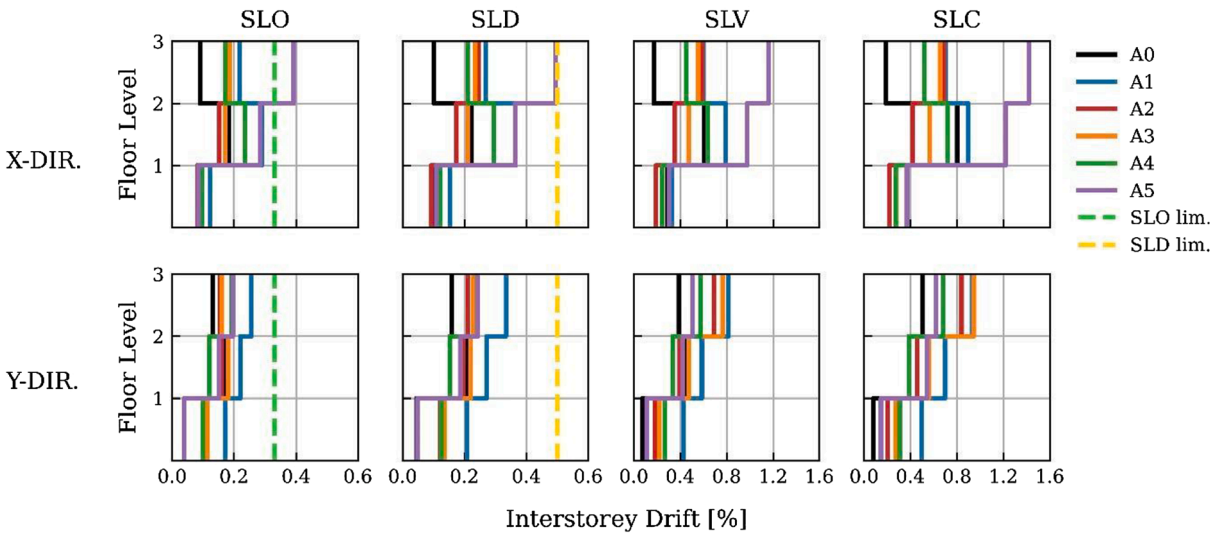

Fig. 9. Drift profiles of the five retrofit alternatives at the N2 displacement demand at SLO, SLD, SLV and SLC. The drift profiles of A0 are provided for comparison.

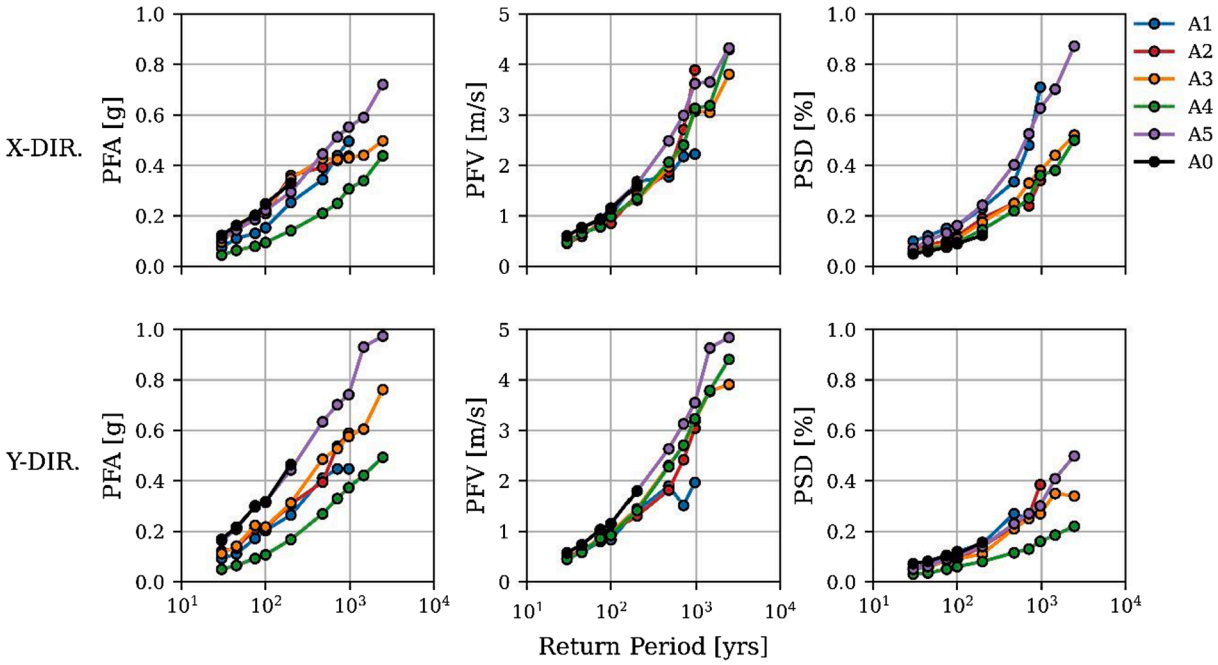

Fig. 10. Median maximum PFA, PFV, and PSD recorded at each intensity level during the MSA.

input in the loss assessment procedure. These vectors account for the aleatory uncertainty inherent in the record-to-record variability of the selected ground motions, but they do not account for the epistemic uncertainty associated with the assumptions made in the development of the numerical models. To account for this, an additional modelling dispersion was considered. In this study, a value of 0.4 was adopted for all structures and EDPs based on the values proposed by O'Reilly and Sullivan [92].

The results from the MSA can also be used to develop collapse fragility curves for A0 and each of the five alternatives, by recording, at each intensity level, the number of collapses observed. A collapse was considered to have occurred if one of the following conditions was met:

1. The shear force demand exceeds the shear resistance of one or more of the beam or column elements;
2. The rotation of one or more of the plastic hinges in the beam, column or wall elements exceeds the SLC deformation limits;
3. The shear deformation in one or more of the BCJ joints exceeds 0.02 rad.

These collapse criteria are similar to those required by the NTC [45]. However, the failure criteria of the BCJs are based on the deformation rather than the strength requirements specified in the code. The reason for this is that the code calculation for maximum joint capacity corresponds roughly to the moment at which the joints begin to crack when using the models proposed by O'Reilly and Sullivan [76]. This is very conservative given that the experimental tests reviewed in that study [76] show that external and internal joints can continue to carry gravity loads when joint strains are as high as 0.02 rad. If the conservative approach was used in this study, a significant number of collapses would have been prematurely recorded and a suitable estimate of the collapse

fragility could not have been obtained with the chosen set of return periods. The collapse fragility curves for the A0 and the five alternatives are presented in Fig. 11. The curves were fitted from the MSA collapse data using a lognormal distribution and maximum-likelihood estimation [93].

As for the demand vectors, the fragility curves obtained from the fitting procedure account for the record-to-record variability of the selected ground motions, but they do not account for the epistemic uncertainty of the numerical models. To account for this additional uncertainty, the median and dispersion values from the fitting procedure were modified following the recommendations of O'Reilly and Sullivan [92]. The median value of A5 was not adjusted, unlike the other four alternatives, as it was assumed that the modelling of the shear walls would have little impact on the median value, in a manner similar to MRFs with infills [92]. As evidenced by Fig. 11, A0 is highly vulnerable to collapse, with the median of the collapse fragility function corresponding to ground motion intensity with a return period of approximately 150 years. The proposed retrofit alternatives all improve the collapse performance of the case-study structure, with significant improvements being shown by A3, A4 and A5.

4.3. Inventory of damageable components

After the characterisation of the structural performance, the next step in the assessment procedure was estimating damage for different levels of structural response. For this purpose, an inventory of damageable components likely to be present in the case-study building was developed. The types of components included in the inventory were adopted from previous seismic assessment studies of Italian RC school buildings [81] which were based on the results of in-situ surveys. The quantities of the non-structural components were estimated by scaling the quantities from O'Reilly et al. [81] by the ratio of the floor areas (and rounding to suitable whole numbers). The quantities of the structural elements and the masonry infills were determined directly from the architectural plans of the case-study building [74] and the design of the retrofit alternatives. The quantities are expressed on either a per m^2 or per unit basis. The important assumptions and calculations performed during the compilation of the component inventory are detailed in the following paragraphs.

The fragility of the retrofitted BCJs and columns was, for simplicity, assumed to be similar to BCJs and columns designed to modern seismic design standards. Although not strictly true, this assumption results in the retrofitted elements suffering significantly less damage than the as-built elements, which is deemed to sufficiently capture the intended effects of the retrofit designs. The fragility of the infills was modelled using the curves proposed by Sassun et al. [67]. For the rest of the non-structural components, the fragility curves were adopted directly from the existing PACT database [49], with the exception of the windows, doors, desks and chairs. In these four cases, it was assumed that the damage to these components would be caused by the collapse of the infills, so the damage states were based on the infill fragility of DS4 adopted from Sassun et al. [67].

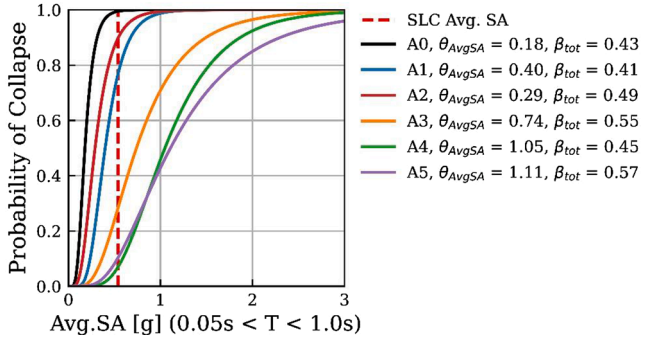

Fig. 11. Collapse fragility functions of A0 and the five retrofit alternatives. The Avg. SA at SLC is indicated by the vertical red line. The median (θ_{AvgSA}) and the total dispersion (β_{tot}) of each fragility curve after accounting for the epistemic uncertainty is indicated in the legend.

The cost consequences for all components are expressed in terms of euros (€) per unit and adjusted for inflation to June 2020. In the cases where the costs were obtained from literature, an appropriate inflation factor was obtained from the Italian national economic statistics between the reference year of the cost (e.g. 2011 for costs obtained from Sassun et al. [67] and 2013 for costs obtained from Cardone [68]) and June 2020. In the cases where the cost data was sourced from the PACT database [49] the cost consequences were adjusted to account for the local labour and material construction cost ratios, inflation and currency exchange rates using the method proposed by Silva et al. [94]. Using this method, an estimate of the fraction of cost associated with labour needs to be made for each repair action. In the absence of more detailed information, the recommendations of Porter et al. [95] were followed to assign labour factors depending on the type of work being carried out. Previous studies [32,73,81] have adopted repair costs for the contents components based on the expert opinion of a local Italian engineering firm. These cost estimates were also adopted in this study and were adjusted to account for the effects of inflation. The inflation factors and currency exchange rates used for adjusting the repair cost consequences obtained from different sources are presented in Table 4.

A point to note is that the masonry infill/partition components have been divided into three different component types depending on the size of the window penetrations in the panel. The reason for this is that the inclusion of windows can significantly increase the costs when the panel is damaged [67]. The costs associated with the repair of these infill elements only considers the costs of the masonry and they have been scaled to reflect the reduced area of masonry per m^2 of panel area.

Similar to the cost consequences, EI consequences of repair were determined using several different methods. The first method was to simply adopt the EI values from the existing PACT database [49] and was applied to components where the cost consequence data was also obtained from the PACT database [49]. The second method was applied to components that had similar damage states and repair requirements to elements already in the PACT database [49] but with different cost consequences, such as the non-ductile BCJs and columns. In this case, the EIs were estimated simply by scaling the database EIs by the ratio of the database repair costs and the adopted repair costs. The final method uses the EEIOLCA calculation procedure illustrated in Fig. 3 and was applied to all components where the two methods described previously could not be applied. The repair costs were disaggregated into the contributing industrial sectors using the authors' judgement. For simplicity, the costs were disaggregated into at most two industrial sectors plus the contribution of labour to the total cost. The sector costs were then used in conjunction with the USEEIO database [66] to determine the EIs. It is worth noting that the estimation of the EIs could be improved if the disaggregation of costs was performed by an experienced cost estimator, as was done for the PACT database [49,55]. In this instance, however, where the results are being used in a

Table 4
Exchange and Inflation rates used to scaling cost data for the calculation of repair cost consequences and environmental impact

Exchange Rates	
USD – Euro (June 2020)	0.889
USD – Euro (2013 avg.)	0.752
USD – Euro (2011 avg.)	0.719
Inflation Rates	
USD (2011–2020)	1.12
USD (2013–2020)	1.10
USD (2011–2013)	1.03
EUR-Italy (2011–2020)	1.10
EUR-Italy (2013–2020)	1.04

comparative study, the effect of this inaccuracy is likely to be small.

4.4. Economic loss and environmental impact estimation

The final phase of the assessment procedure is the loss estimation. The results from the previous sections were combined into a building performance model that can be used with PACT [49] to estimate the expected economic and environmental impacts due to seismic hazard. In addition to the economic and environmental consequences outlined in Section 4.3, an estimate of the replacement costs and EIs was required so that losses associated with collapse of the structures could be incorporated into the assessment. Data from past earthquakes in the Italian region was used to estimate the demolition and replacement costs. Following the Emilia Romagna earthquakes in 2012, the average costs of building demolition and reconstruction were 95.50 €/m^2 and 1805.75 €/m^2, respectively [81], for a total of 1901.25 €/m^2. These values were adopted in the present study for the calculation of replacement costs and EIs. Given an approximate floor area of 1395 m^2 the demolition and reconstruction costs were estimated to be 133,222 € and 2,519,020 € respectively, for a total replacement cost of 2,652,242 €. The reconstruction EIs were coarsely approximated by first converting the reconstruction cost, in 2020 €, to 2013 USD, then multiplying the reconstruction cost by the EIs/€ factor for "schools and vocational buildings" from the USEEIO database [66]. An additional 15% of the reconstruction EI was added to account for the impacts associated with the demolition and disposal of the damaged structure. This assumption is consistent with previous studies made in this field [40,43] and is reasonable for Italian buildings if only moderate levels of recycling are considered [96]. These calculations and assumptions resulted in a replacement EI of 1,830,000 kgCO_2e. For simplicity, the repair costs and EIs were considered to be the same for all of the alternatives. In addition to the replacement cost estimates, a threshold above which the losses are deemed so significant that the owner would opt to demolish rather than repair the building also needs to be specified. This study adopted a loss ratio of 60% of the total building cost, in line with observations made by Cardone and Perrone [1] following the 2016 L'Aquila earthquake. Additionally, the probability that the building would be demolished as a result of significant residual displacements was considered assuming a fragility curve with a mean of 1.5% drift and a dispersion of 0.3 [81].

The results of the loss assessment are presented in Fig. 12 and Table 5. Fig. 12 displays the vulnerability curves for the expected economic and environmental losses for each return period, as a fraction of the total replacement cost. From these plots, it is evident that A0 is extremely vulnerable and that collapse plays a significant role in the expected losses of the structure compared to the retrofitted alternatives. There is clearly a substantial improvement in the expected losses of alternatives A3, A4, and A5 for ground motions with longer return periods. This can be attributed to the combined effect of the additional lateral load resisting elements and the increased strength and deformation capacity of the existing elements. In these three cases, the economic losses and EIs at SLV and SLC vary between 5% and 15% and 7.5% and25% of the replacement cost, respectively. Conversely, the performance of A1 and A2, whilst better than A0, is still significantly affected by collapse, as evidenced by the significant increase in expected losses from around 10% of the replacement cost at a 475-year return period to almost 100% of the replacement cost at a 712-year return period.

Table 5
Expected annual economic losses and EIs expressed as a percentage (%) of the estimated replacement cost and EI.

	EAL	Repl. Cost [€]	EAEI	Repl. EI [kgCO_2e]
A0	0.50%	2,652242	0.51%	1,830,00
A1	0.20%		0.18%	
A2	0.43%		0.39%	
A3	0.16%		0.11%	
A4	0.06%		0.04%	
A5	0.13%		0.10%	

The economic expected annual loss (EAL) for A0 was 0.5% of the total replacement cost of the building. This estimate is considered reasonable for pre-1970s Italian RC structures given that it falls close to the values obtained by other studies on similar buildings [28,81]. As observed in Table 5, all of the alternatives have reduced EALs when compared to A0. A1, A3 and A5 have all produced reductions in EAL in the range of 60–75%, whereas A4, the alternative incorporating supplemental damping and FRP strengthening, has seen a reduction of 88%. This excellent performance is due to the reduced PFAs and PSDs resulting from the additional damping. In contrast, A2, which utilises steel braces, exhibits only a minor improvement in EAL of 14%. This poor performance can be attributed to the inability of the steel braces to prevent the collapse of the structure due to shear failure of the column and beam members.

From the results of the structural analyses and loss assessments presented in this section, it is clear that several of the proposed retrofit alternatives outperform other alternatives by a significant margin. However, there are many other criteria, as already mentioned, that can be considered in a comprehensive selection process. The following section will describe in detail the various decision criteria employed in this study, use them to perform an MCDM assessment to select the 'optimal' retrofit solution considering the specified criteria and investigate how the consideration or not of EIs can affect the result.

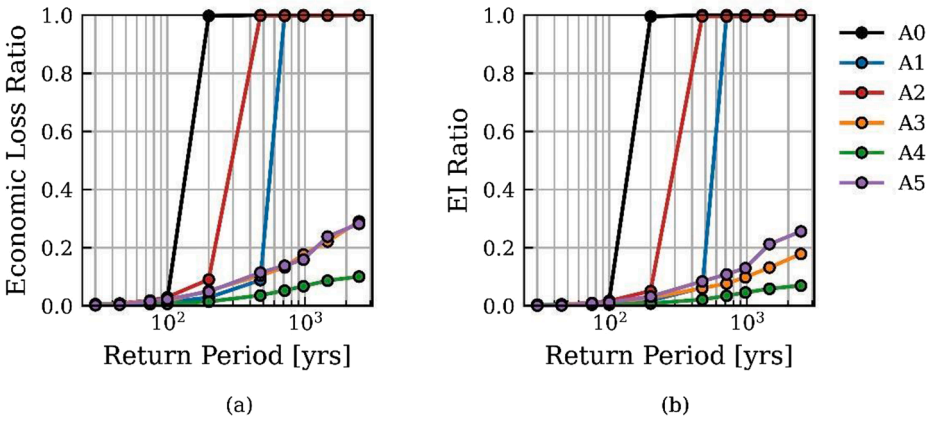

Fig. 12. Vulnerability curves for A0 and the five alternatives: (a) Economic vulnerability; (b) Environmental vulnerability.

5. Selection of the optimal retrofit alternative

5.1. Determination of the decision matrix values and weight vectors

In this section, the selection of the optimal retrofitting alternative will be made using different combinations of DVs to investigate how the consideration of EIs in the MCDM process can affect the ranking. The DVs considered in this study are described in the following paragraphs. The specific values of each DV for the five alternatives are presented in Table 6. Fig. 15 presents the values of the DVs, normalised by the largest value, for a visual comparison.

C_1 Installation Costs: The total cost of installation of each retrofit alternative considers the removal of internal linings, partial demolition of the existing structure/infills as required, removal of debris, installation of the retrofit scheme, and restoration of infills and linings as required. Costs associated with the installation of CFRP or steel braces were generally based on the data provided in Mazzolani et al. [14] and scaled based on the quantities of material required. The costs associated with the installation of the RC walls were estimated using data obtained from the American Society of Professional Estimators [97] and adjusting the final value using the recommendations of Silva et al. [94]. The cost of the steel joint enlargement was estimated simply by multiplying the weight of the steel required by the average cost of hot-rolled steel products in Europe, as of June 2020. The cost of the dampers was obtained directly from a local manufacturer in Italy.

C_2 Maintenance Costs: The cost of maintenance over the lifetime of the structure (75 years) was obtained by considering the interventions outlined by Caterino et al. [30] and scaling them based on the quantity of materials used. An inflation rate of 1% per year was considered in these calculations.

C_3 Duration of Works: The data presented by Mazzolani et al. [14] was used to estimate the duration of the intervention works for structures with CFRP or steel braces. The values from Mazzolani et al. [14] were scaled based on material quantities and floor area where appropriate. It was also assumed that a maximum of 20 workers is present on site at a given time. The estimate of the construction time of the RC walls was calculated using the method detailed by Hofstadtler [98] and the production rate data adapted from [97]. In light of a lack of available information, it was assumed that 4 workers can install 16 steel joint systems per day.

C_4 Architectural Impact: The qualitative ranking of the alternatives based on their architectural impact was performed using the AHP, as described by Caterino et al. [30]. In this method, a series of pairwise comparisons are made between the retrofit alternatives in which the impact of Alternative A is compared to Alternative B and an integer value assigned on the range 1–9. A value of 1 indicates that the impact of both alternatives is exactly the same, whereas 9 indicates that Alternative A has a significantly larger impact than Alternative B. In the case where Alternative B is compared to Alternative A, the reciprocal value of the first comparison is used. Once all of the comparisons have been performed and combined into a preference matrix, the weight vector ranking each of the alternatives by their architectural impact can be determined. See the work of Caterino et al. [30] for an easy step-by-step implementation of this method. The preference matrix used in this study was based on the professional judgement of the authors.

C_5 Need for Specialised Labour: The values for this variable were determined using the AHP and the judgement of the authors in a procedure analogous to C_4.

C_6 Foundation Intervention: The values for this variable were determined using the AHP. In this case, the judgement of the authors was supplemented by estimates of the axial loads on the foundations and the approximate volume of concrete required for new foundations.

C_7 Economic Losses at SLD and **C_8 Economic Losses at SLV**: These values were obtained from the lost estimation results presented in Fig. 12.

C_9 Installation EIs: The EIs associated with the installation of the retrofit alternatives were estimated using the EEIOLCA procedure described previously (and shown in Fig. 3). Each component of the installation cost was disaggregated into the appropriate industrial sectors and used in conjunction with the USEEIO database [66] to estimate the EIs.

C_{10} Expected Annual EIs and **C_{11} Expected Annual Losses**: The values for the EAEIs and EAL are obtained from the results of the loss assessment presented in Table 6.

C_{12} Environmental LCPM and **C_{13} Economic LCPM**: The values of these LCPMs were calculated using Equation (2),

$$LCPM = \frac{IC + EAL_{post-retrofit} \times SL + MC}{A \times SL} \tag{2}$$

where IC is the installation cost (economic or environmental) of the retrofit alternative, $EAL_{post-retrofit}$ is the EAL of the retrofitted structure, SL is the expected service life of the structure post-retrofit, MC is the total maintenance cost of the alternative over the expected service life, and A is the total floor area of the building. This has been proposed by Caruso et al. [44] to include the maintenance costs of each solution and remove the consideration of the pre-retrofit phase as this will be the same for all of the buildings. The units of these variables can be expressed in terms of € or $kgCO_2e$ depending on the LCPM desired. A service life of 75 years was chosen based on the nominal building life specified in the NTC [45].

Using the values of the DV summarised in Table 6, a collection of smaller decision matrices can be developed to investigate how different combinations of variables affect the order of preference of the alternatives. A total of six different combinations of DVs were investigated and each of them are summarised in Table 7, along with the corresponding weight vector values.

The decision matrices can be divided into two main sets. In Set One, which comprises D_A, D_B, D_C and D_D, the matrices contain several different economic DVs (C_1, C_2, C_7, and C_8), each of which have been assigned specific weight values. Contrastingly, in Set Two, which

Table 6
Decision Matrix Values used in the MCDM Assessment.

Variable		Unit	A1	A2	A3	A4	A5
C_1	Installation cost	€	850,458	43,120	389,477	679,445	508,018
C_2	Maintenance cost	€	1,520,883	229,829	794,218	810,781	2,137,838
C_3	Duration of works	Days	36	8	28	29	40
C_4	Architectural Impact	–	0.05	0.16	0.24	0.43	0.11
C_5	Need for specialised labour	–	0.24	0.03	0.22	0.40	0.10
C_6	Need for foundation intervention	–	0.06	0.22	0.22	0.03	0.47
C_7	Economic losses at SLD	€	26,296	45,000	41,500	14,818	43,666
C_8	Economic losses at SLV	€	2,511,228	2,513,377	332,500	131,818	337,272
C_9	Installation EIs	$kgCO_2e$	465,123	67,551	240,976	299,411	225,848
C_{10}	EAEI	$kgCO_2e$	3,385	7,512	2,190	754	1,890
C_{11}	EAL	€	5,247	11,403	4,228	1,587	3,428
C_{12}	LCPM – € 75yrs	€/m^2/yr.	22.00	10.29	12.05	13.05	21.34
C_{13}	LCPM – Env. 75yrs	$kgCO_2e$/ m^2/yr.	7.04	6.27	4.06	3.67	4.21

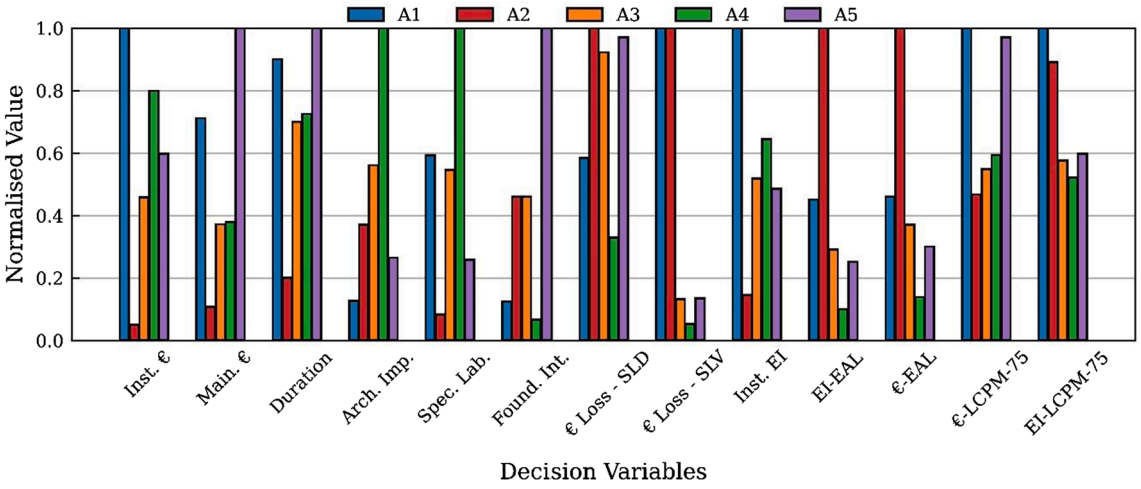

Fig. 15. Normalised decision matrix values for the five alternatives considered in the MCDM assessment.

Table 7
Summary of the DVs included in each of the five decision matrices. The numbers contained in each cell indicate the weight assigned to that particular DV for that analysis. DVs indicated with grey cells were not included in a particular analysis.

		Decision Matrices					
Decision Variable		**D_A**	**D_B**	**D_C**	**D_D**	**D_E**	**D_F**
C_1	Installation Cost	0.133	0.119	0.119	0.119		
C_2	Maintenance Cost	0.138	0.123	0.123	0.123		
C_3	Duration of Works	0.120	0.108	0.108	0.108	0.226	0.189
C_4	Architectural Impact	0.105	0.094	0.094	0.094	0.202	0.166
C_5	Specialised Labour	0.108	0.097	0.097	0.097	0.176	0.169
C_6	Foundation Intervention	0.127	0.113	0.113	0.113	0.182	0.147
C_7	€ Losses SLD	0.133	0.119	0.119	0.119		
C_8	€ Losses SLV	0.135	0.121	0.121	0.121		
C_9	Installation EIs		0.106				
C_{10}	EAEI				0.106		
C_{11}	EAL						
C_{12}	LCPM € - 75yrs					0.213	0.152
C_{13}	LCPM EI – 75yrs			0.106			0.178

comprises D_D, and D_E, the four economic variables have been aggregated into a single LCPM. Matrix D_A, adopted from the work of Carofilis et al. [73], represents the baseline option for this study as it contains decision-making criteria that are commonly considered when retrofitting structures focusing just on seismic aspects without any EI variables. Matrices D_B, D_C and D_D build on D_A by adding an environmental variable to the analysis. D_B considers EIs using the installation EIs as the environmental variable, whilst D_C considers the total LCEIs through the environmental LCPM. D_D uses the EAEI as the EI DV. A comparison of the results of these four assessments will provide insight into whether or not and in which way the inclusion of EIs can affect the preferential ranking of the alternatives. Matrix D_E is another assessment scenario that does not include EIs, however, it differs from D_A by condensing all of the cost-related variables into the single economic LCPM variable. Matrix D_F extends the assessment of D_E with the inclusion of the environmental LCPM.

The values of the weight vector for each decision matrix were determined simply by renormalising the mean weights obtained from the survey conducted by Carofilis et al. [73] depending on which variables were included in the assessment. In the case of the economic

LCPM, the weight was assumed to be the average of the weights of the contributing variables (C_1, C_2, C_7, and C_8).

5.2. Selection results

The decision matrices and weight vectors presented in the previous section were used as inputs in the MCDM procedure introduced in Section 4. The preferential rankings obtained from each analysis are presented in Table 8, where the alternative in position **I** is considered the most preferred alternative, given the selection criteria and weights, and the alternative in position **V** is the least preferred option. The bracketed values indicate the relative closeness of each alternative to the fictitious 'ideal' retrofit alternative, a parameter used to rank the alternatives in preferential order. The relative closeness values lie in the range (0,1), with a value of 1 indicating that an alternative is the 'ideal' solution. The difference between the relative closeness values can be used to understand how strongly one solution is preferred over another.

Considering Set 1, it is clear that there is a slight preference for A2 to be ranked in the first position with a difference between the **I** and **II** alternatives ranging between 1.8% and 7%, depending on the decision matrix considered. The preference of A2 despite its poor seismic performance (Fig. 15), can be attributed to the extremely low installation and maintenance costs which out-perform all of the other alternatives by a significant margin. In contrast, A5 and A1 are the least preferred alternatives. The low ranking of A5 can be attributed primarily to its high maintenance costs and the level of intervention required at the foundation level. A1, on the other hand, is hampered by high installation costs and SLV losses. Unlike A2, A5 and A1 do not significantly outperform the rest of the alternatives for any DV, resulting in a low preferential ranking.

Comparing the results of D_B, D_C, and D_D to D_A it is clear that the inclusion of EIs in the MCDM framework can alter the preferential ranking of the retrofit alternatives. In the case of D_B practically no significant change occurs in the ranking because the preferred alternative already has the lowest installation EIs, thus, the preference for selecting A2 as the optimal retrofitting alternative is strengthened. This is confirmed by the increase in the difference between the relative closeness values of **I** and **II** from the D_B analysis compared to those from D_A. A small change is observed in the alternatives ranked **IV** and **V**. In the case of D_C, A2 remains the preferred solution but the strength of the preference is reduced because A2 has a higher environmental LCPM than either of the alternatives ranked **II** and **III**. For the D_D analysis, A3 and A4 are the preferred alternatives, whilst A2 is ranked **III**. The drop in ranking of A2 is directly attributed to the fact that this alternative has the worst EAEI performance. Unlike D_C, the installation EIs are not included in this assessment so the low installation EIs of A2 cannot offset the high EAEI.

Table 8
Rankings of the retrofit alternatives in order of preference following the MCDM assessments. The relative closeness of each alternative is indicated by values in parentheses.

D Matrix		Alternative Ranking				
		I	**II**	**III**	**IV**	**V**
Set 1	D_A	A2 (0.609)	A3 (0.586)	A4 (0.542)	A1 (0.458)	A5 (0.435)
	D_B	A2 (0.628)	A3 (0.584)	A4 (0.534)	A5 (0.445)	A1 (0.433)
	D_C	A2 (0.602)	A3 (0.591)	A4 (0.547)	A1 (0.452)	A5 (0.441)
	D_D	A3 (0.610)	A4 (0.577)	A2 (0.547)	A5 (0.473)	A1 (0.473)
Set 2	D_E	A2 (0.737)	A1 (0.612)	A3 (0.536)	A4 (0.484)	A5 (0.417)
	D_F	A2 (0.709)	A1 (0.591)	A3 (0.550)	A4 (0.497)	A5 (0.348)

Given that the inclusion of an EI DV can have an impact on the ranking of the alternatives, it is important, therefore, that the appropriate EI DV be chosen. As the previous analyses have alluded to, there are several parameters that may be considered, such as the installation EIs, EAEIs or the total LCEIs. When calculating the EIs of a structure the emphasis tends to be on estimating total LCEIs. It follows then that the most applicable EI DV that can be included in the decision analysis is the LCPM or a similar variable that is capable of capturing all of the sources of EI over a structure's life. However, calculating the initial and maintenance components of the environmental LCPM can be time-consuming and require specialist knowledge of LCA that many structural or earthquake engineers are not familiar with. On the other hand, the calculation of the EIs associated with seismic damage is more immediate, given that extensive EI data is already available in the fragility libraries provided with software such as PACT [45]. To promote the inclusion of EIs in MCDM frameworks, it would be advantageous to only have to rely on EI DVs that are easy to calculate, such as the EAEI. The results of this particular case-study have shown that when the EAEI is used as the EI DV the relative rankings of most of the alternatives remain unchanged. It would appear then, that using the EAEI as the EI DV could be a suitable substitute for the more complex LCPM. However, it should be noted that using the EAEI in lieu of the environmental LCPM can severely disadvantage alternatives that have relatively low installation costs and relatively high EAEI, as was the case for A2 in this study.

Considering Set 2, the same preference for A2 to be ranked **I** can be observed, although in this set it is much stronger. The difference in relative closeness between the alternatives ranked **I** and **II** is approximately 17%. When EIs are considered in D_F the ranking of the alternatives is not affected.

In this set of analyses, the stronger preference for A2 to be ranked **I** compared to the results of Set 1 can be attributed to the use of the economic LCPM, which is an aggregated performance metric, in lieu of the four separate economic parameters, C_1, C_2, C_7, C_8. While useful for providing a comparison between the total life-cycle costs, if that is what is most important, the aggregation of all the economic parameters may not be the best option if a comprehensive decision-making procedure like MCDM is being used. Consider only the economic variables C_1, C_{11} and C_{12}. In this study, the values of C_{12} for A2 and A3 (10.29 €/yr. and 12.05 €/yr., respectively) vary by only ~17%. If only the values of C_{12} were compared it would seem that there is not a huge difference between choosing either A2 or A3 as the preferred alternative, however, upon closer examination, the values of the variables that contribute to the LCPM are quite different. The installation cost (C_1) of A2 is € 346,357 less than A3, or only 11% of the cost of A3, whereas the EAL (C_{11}) for A3 is 37% of that for A2 (4228 €/yr. and 11403 €/yr., respectively). By using the LCPM in this instance, the ability to tailor the weights of different cost variables to the needs of the decision-maker is lost. For example, A2 could be the preferred solution in a situation where limited capital resources are available to retrofit the building, whereas, in the opposite conditions, a decision-maker seeking a low damage design and low on-going costs would prefer A3. Using the LCPM as the only economic variable does not allow one to make these distinctions.

In both the Set 1 and Set 2 analyses there were cases where the inclusion of the EIs did not affect the ranking of the alternatives in any meaningful way. This, naturally, can question the consideration of the EIs in the decision analysis when selecting an optimal retrofit scheme. The answer is not straightforward and depends on several factors. The first factor to be considered is the dispersion of the values of the EI DV between the alternatives. In this particular case-study, a relatively uniform weight vector was used in the decision analysis which means that the variation in the DV values must be large in order to effect some change in the overall rankings, because a uniform weight vector has an averaging effect on the values of the decision matrix. This effect was particularly evident in this study in the results of Set 1. The variation in the values of environmental LCPM (D_C) was not sufficient to cause a change in rankings; however, when EAEIs were used (D_D) the larger

spread in the values caused a ranking change to occur. This observation is only valid for this particular case-study structure and set of retrofit alternatives, as it is very possible that given a different structure and/or a different set of retrofit alternatives simply changing the dispersion of EI DV values would result in a different outcome.

The second, and probably the most important factor, that must be considered when deciding whether or not it is worth considering EIs in the MCDM framework is the weight, or relative importance that will be assigned to the EI DV. It was a key observation in the work of Carofilis et al. [73] that given a range of different sources of uncertainty in the MCDM assessment procedure the factor that had the most significant impact on the results of the assessment was the values of the weight vector. As previously discussed, a uniform weight vector effectively averages the results of a number of DVs, whereas a more skyline profile promotes and demotes various DVs and will likely result in a different ranking. To illustrate this, Fig. 14 presents a comparison between the weight vector used in this study for D_A and one used in a recent MCDM assessment by Gentile and Galasso [31]. The weight vector used by Gentile and Galasso [31] places much more emphasis on the installation cost, seismic losses and intervention at the foundation relative to the rest of the DVs when compared to the vector in this study. Performing an MCDM assessment using the vector from Gentile and Galasso [31], the results of which are compared with those from D_A in Table 9, it is clear that the ranking has changed. Although this comparison has been made with weight vectors that do not include the EI, it can easily be concluded that if a weight vector was used that gave preference to the environmental variables similar results would be expected. Based on this observation, if a weight vector incorporating EIs and considering them to be relatively important compared to some of the other DVs was used in this study then it is likely that the change in the rankings of the D_C and possibly D_E analyses would occur, although this cannot be stated for certain. What this illustrates then, is that it is the preferences of the decision-makers that have the most influence on whether or not the inclusion of EIs alters the ranking of the retrofit alternatives. This also further highlights the utility of the MCDM methodology and its robustness in adapting to different scenarios or priorities.

6. Conclusions

This paper has investigated how environmental impacts (EIs) can be considered in a multi-criteria decision making (MCDM) framework for the selection of optimal retrofitting techniques for an existing reinforced concrete frame school building. Various EI assessment methodologies were discussed and the method adopted in this study, Environmentally Extended Input-Output Life Cycle Analysis (EEIOLCA) was described in detail. A set of five retrofit alternatives were developed using response estimates from non-linear static analyses and their performance was assessed using non-linear time-history analysis and the PEER-PBEE framework. EEIOLCA was used to develop estimates of the EIs

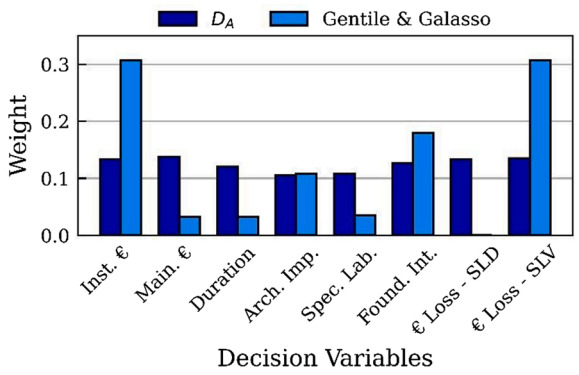

Fig. 14. Comparison of the weight vectors used in this study and the study of Gentile and Galasso [31].

Table 9
comparison of rankings obtained using the weight vectors for D_A and from the study of Gentile and Galasso [31].

	I	II	III	IV	V
D_A	A2 (0.609)	A3 (0.586)	A4 (0.542)	A1 (0.458)	A5 (0.435)
Gentile and Galasso [31]	A3 (0.678)	A4 (0.590)	A5 (0.541)	A2 (0.510)	A1 (0.348)

associated with the installation of the retrofit interventions, repair of seismic damage, and general maintenance. To perform the calculations, a life cycle inventory (LCI) was developed which comprises information obtained from the FEMA Performance Assessment and Calculation Tool (PACT) database and calculations based on cost estimates of the expected work. Several MCDM assessments were conducted each considering a subset of 13 possible decision variables (DVs) to select an optimal retrofitting alternative. The results of the MCDM assessment and their implications were discussed in detail and the main conclusions that can be drawn from this study are:

- The EIs associated with the installation, maintenance and seismic damage can all be determined using the EEIOLCA methodology and cost information readily available to the designer of the retrofit solutions. These can be used to estimate the total life cycle EIs (LCEIs) of the structure;
- When incorporating the EIs into the MCDM framework, the selection of an appropriate EI DV is important as it can affect the ranking of the alternatives. It is recommended that the EI life cycle performance metric (LCPM) or a similar variable that captures the entire life cycle impacts is adopted as the EI DV because it is the most rigorous approach for considering EIs. This DV was also the one causing more changes in the ranking of the different retrofit alternatives;
- To simplify the calculation of the EIs, EAEIs could be used as a substitute for the LCPM in certain cases. This approximation is likely to be more suitable in cases where the EAEIs of all the alternatives is of a similar magnitude as it disadvantages alternatives with comparatively low seismic performance, even if their overall LCEIs are not significantly different from the other alternatives;
- There are positive and negative aspects of aggregated performance metrics, such as the LCPM, that should be considered when selecting DVs for use in the MCDM framework. The analyst should consider carefully whether or not aggregated performance metrics sufficiently describe the information that is available to make the decision. Aggregated economic metrics may thus be of limited use in an MCDM framework that, in the context of seismic retrofitting, commonly considers several different economic parameters. Using an aggregated economic metric limits the ability of the decision-maker to assign different weights to the constituent variables (installation costs, maintenance costs, seismic losses, etc) meaning that the assessment cannot be tailored to suit the financial resources they have available. Conversely, aggregated EI metrics are a much more practical option for considering the LCEIs, as there is no clear benefit to be had in considering the constituent variables (EIs from installation, seismic repair, maintenance, etc) separately. Additionally, in the case of the LCEIs little guidance is available to help determine weights for each of the constituent variables and considering a single DV with one weight reduces the associated uncertainty;
- The most important factor in determining the influence of the EI DV on the ranking of the alternatives is likely to be the DV weight provided by the decision-maker. These weights can be determined in a number of ways such as personal preference, the analytical hierarchy process (AHP) or from the results of a survey, amongst others. Ultimately, all these methods are suitable if the weights they produce are acceptable to the decision-maker;

- The procedure implemented in this study to select an optimal retrofit alternative for an existing building is somewhat time-consuming and computationally intensive given the need to perform a large number of NLTHAs and individual LCAs for each retrofit alternative. To make this methodology more attractive to practising engineers, future research will focus on simplifying aspects of this procedure to make it more accessible and time-efficient. In addition to using EAEI in lieu of the complete LCA, possible branches of investigation include checking if using a component-based loss assessment, such as the one performed in this study, with results from non-linear pushover analyses, or simplified loss assessment techniques, such as the Italian seismic risk assessment guidelines (Sismabonus), produce similar results to the detailed approach described herein.

CRediT authorship contribution statement

Nicholas Clemett: Methodology, Validation, Formal analysis, Writing – original draft, Writing – review & editing, Visualization. **Wilson Wladimir Carofilis Gallo:** Methodology, Validation, Formal analysis, Writing – review & editing. **Gerard J. O'Reilly:** Methodology, Writing – review & editing. **Giammaria Gabbianelli:** Methodology, Writing – review & editing. **Ricardo Monteiro:** Conceptualization, Methodology, Writing – review & editing, Supervision, Project administration.

Declaration of Competing Interest

The authors declare that they have no known competing financial interests or personal relationships that could have appeared to influence the work reported in this paper.

Acknowledgements

This work has been developed within the framework of the project "Dipartimenti di Eccellenza", funded by the Italian Ministry of Education, University and Research, and ReLUIS 2019-2021, funded by the Italian Department of Civil Protection.

References

[1] Cardone D, Perrone G. Damage and Loss Assessment of Pre-70 RC Frame Buildings with FEMA P-58. J Earthq Eng 2017;21:23–61. https://doi.org/10.1080/13632469.2016.1149893.
[2] Calvi GM. Choices and Criteria for Seismic Strengthening. J Earthq Eng 2013;17:769–802. https://doi.org/10.1080/13632469.2013.781556.
[3] European Commission. Energy-efficient buildings: multi annual roadmap for the contractual PPP under Horizon 2020; 2013.
[4] Deloitte. Resource efficient use of mixed wastes: Improving management of construction and demolition waste. European Commission DG ENV; 2017.
[5] Applied Technology Council. ATC-40 seismic evaluation and retrofit of concrete buildings. Applied Technology Council; 1996.
[6] Del Vecchio C, Di Ludovico M, Prota A, Manfredi G. Analytical model and design approach for FRP strengthening of non-conforming RC corner beam–column joints. Eng Struct 2015;87:8–20. https://doi.org/10.1016/j.engstruct.2015.01.013.
[7] Akguzel U, Pampanin S. Assessment and Design Procedure for the Seismic Retrofit of Reinforced Concrete Beam-Column Joints using FRP Composite Materials. J Compos Constr 2012;16:21–34. https://doi.org/10.1061/(ASCE)CC.1943-5614.0000242.
[8] Fardis MN. Seismic Design, Assessment and Retrofitting of Concrete Buildings based on EN-Eurocode 8. vol. 8. Dordrecht: Springer Netherlands; 2009. https://doi.org/10.1007/978-1-4020-9842-0.
[9] Karayannis CG, Chalioris CE, Sirkelis GM. Local retrofit of exterior RC beam–column joints using thin RC jackets—An experimental study. Earthq Eng Struct Dyn 2008;37:727–46. https://doi.org/10.1002/eqe.783.
[10] Tsonos A-DG. Performance enhancement of R/C building columns and beam–column joints through shotcrete jacketing. Eng Struct 2010;32:726–40. https://doi.org/10.1016/j.engstruct.2009.12.001.
[11] Shafaei J, Hosseini A, Marefat MS. Seismic retrofit of external RC beam–column joints by joint enlargement using prestressed steel angles. Eng Struct 2014;81:265–88. https://doi.org/10.1016/j.engstruct.2014.10.006.
[12] Tsionis G, Taucer F, Pinto A. Seismic strengthening of rc frames with shear walls. Proc. 6th Int. Conf. Mech. Mater. Des., P. Delgada, Azores; 2015, p. 12.
[13] Mahrenholtz C, Lin P-C, Wu A-C, Tsai K-C, Hwang S-J, Lin R-Y, et al. Retrofit of reinforced concrete frames with buckling-restrained braces. Earthq Eng Struct Dyn 2015;44:59–78. https://doi.org/10.1002/eqe.2458.
[14] Mazzolani FM, Formisano A, Vaiano G. Adeguamento sismico di edifici in cemento armato: BRB e FRP. Costr Met 2018:26.
[15] Christopoulos C, Filiatrault A. Principles of Passive Supplemental Damping and Seismic Isolation. IUSS Press Pavia 2006.
[16] Pettinga D. Retrofit of Reinforced Concrete Moment Frames in NZ Using Dual Supplemental Damping. Struct Eng Int 2020;30:185–91. https://doi.org/10.1080/10168664.2020.1711849.
[17] Mazza F, Mazza M, Vulcano A. Base-isolation systems for the seismic retrofitting of r.c. framed buildings with soft-storey subjected to near-fault earthquakes. Soil Dyn Earthq Eng 2018;109:209–21. https://doi.org/10.1016/j.soildyn.2018.02.025.
[18] Grossi E, Zerbin M, Aprile A. Advanced Techniques for Pilotis RC Frames Seismic Retrofit: Performance Comparison for a Strategic Building Case Study. Buildings 2020;10:149–78. https://doi.org/10.3390/buildings10090149.
[19] Seo H, Kim J, Kwon M. Optimal seismic retrofitted RC column distribution for an existing school building. Eng Struct 2018;168:399–404.
[20] Falcone R, Carrabs F, Cerulli R, Lima C, Martinelli E. Seismic retrofitting of existing rc buildings: a rational selection procedure based on genetic algorithms. Structures 2019;22:310–26.
[21] Papavasileiou GS, Charmpis DC, Lagaros ND. Optimized seismic retrofit of steel-concrete composite buildings. Eng Struct 2020;213:110573.
[22] Di Trapani F, Malavisi M, Marano GC, Sberna AP, Greco R. Optimal seismic retrofitting of reinforced concrete buildings by steel-jacketing using a genetic algorithm-based framework. Eng Struct 2020;219:110864.
[23] Cimellaro GP. Resilience-based design (RBD) modelling of civil infrastructure to assess seismic hazards. Handb Seism Risk Anal Manag Civ Infrastruct Syst, Elsevier 2013:268–303. https://doi.org/10.1533/9780857098986.2.268.
[24] Cimellaro GP. Seismic resilience of a regional system of hospitals. In: Dogreul S, Retamales R, editors. Stud. Res. Accompl. 2006-2007, University at Buffalo, New York, USA: MCEER; 2007, p. 3–7.
[25] Hadigheh SA, Mahini SS, Setunge S, Mahin SA. A preliminary case study of resilience and performance of rehabilitated buildings subjected to earthquakes. Earthq Struct 2016;11:967–82. https://doi.org/10.12989/EAS.2016.11.6.967.
[26] Requena-García-Cruz M-V, Morales-Esteban A, Durand-Neyra P, Estêvão JMC. An index-based method for evaluating seismic retrofitting techniques. Application to a reinforced concrete primary school in Huelva. PLOS ONE 2019;14:e0215120. https://doi.org/10.1371/journal.pone.0215120.
[27] Cardone D, Gesualdi G, Perrone G. Cost-Benefit Analysis of Alternative Retrofit Strategies for RC Frame Buildings. J Earthq Eng 2019;23:208–41. https://doi.org/10.1080/13632469.2017.1323041.
[28] Sousa L, Monteiro R. Seismic retrofit options for non-structural building partition walls: Impact on loss estimation and cost-benefit analysis. Eng Struct 2018;161:8–27. https://doi.org/10.1016/j.engstruct.2018.01.028.
[29] Williams RJ, Gardoni P, Bracci JM. Decision analysis for seismic retrofit of structures. Struct Saf 2009;31:188–96. https://doi.org/10.1016/j.strusafe.2008.06.017.
[30] Caterino N, Iervolino I, Manfredi G, Cosenza E. Multi-Criteria Decision Making for Seismic Retrofitting of RC Structures. J Earthq Eng 2008;12:555–83. https://doi.org/10.1080/13632460701572872.
[31] Gentile R, Galasso C. Shedding some light on multi-criteria decision making for seismic retrofitting of RC buildings. London: Greenwich; 2019. p. 10.
[32] Carofilis W, Gabbianelli G, Monteiro R. Assessment of multi-criteria evaluation procedures for identification of optimal retrofitting strategies for existing RC buildings. J Earthquake Eng 2021. https://doi.org/10.1080/13632469.2021.1878074.
[33] USGBC. LEED rating system | U.S. Green Building Council. US Green Build Counc; 2021. https://www.usgbc.org/leed [accessed February 11, 2021].
[34] BRE. BREEAM: the world's leading sustainability assessment method for masterplanning projects, infrastructure and buildings. BREEAM 2021. https://www.breeam.com/ [accessed February 10, 2021].
[35] Feese C, Li Y, Bulleit WM. Assessment of Seismic Damage of Buildings and Related Environmental Impacts. J Perform Constr Facil 2015;29:04014106. https://doi.org/10.1061/(ASCE)CF.1943-5509.0000584.
[36] Comber MV, Poland C, Sinclair M. Environmental Impact Seismic Assessment: Application of Performance-Based Earthquake Engineering Methodologies to Optimize Environmental Performance. Struct. Congr. 2012, Chicago, Illinois, United States: American Society of Civil Engineers; 2012, p. 910–21. https://doi.org/10.1061/9780784412367.081.
[37] Padgett JE, Li Y. Risk-Based Assessment of Sustainability and Hazard Resistance of Structural Design. J Perform Constr Facil 2016;30:04014208. https://doi.org/10.1061/(ASCE)CF.1943-5509.0000723.
[38] Lippiatt BC. Building for Environmental and Economic Sustainability Technical Manual and User Guide. National Institute of Standards and Technology; 2007.
[39] Hossain KA, Gencturk B. Life-Cycle Environmental Impact Assessment of Reinforced Concrete Buildings Subjected to Natural Hazards. J Archit Eng 2016;22. https://doi.org/10.1061/(ASCE)AE.1943-5568.0000153.
[40] Gencturk B, Hossain K, Lahourpour S. Life cycle sustainability assessment of RC buildings in seismic regions. Eng Struct 2016;110:347–62. https://doi.org/10.1016/j.engstruct.2015.11.037.
[41] Wei H-H, Skibniewski MJ, Shohet IM, Yao X. Lifecycle Environmental Performance of Natural-Hazard Mitigation for Buildings. J Perform Constr Facil 2016;30:04015042. https://doi.org/10.1061/(ASCE)CF.1943-5509.0000803.
[42] Wei H-H, Shohet IM, Skibniewski MJ, Shapira S, Yao X. Assessing the Lifecycle Sustainability Costs and Benefits of Seismic Mitigation Designs for Buildings.

J Archit Eng 2016;22:04015011. https://doi.org/10.1061/(ASCE)AE.1943-5568.0000188.
[43] Chiu CK, Chen MR, Chiu CH. Financial and Environmental Payback Periods of Seismic Retrofit Investments for Reinforced Concrete Buildings Estimated Using a Novel Method. J Archit Eng 2013;19:112–8. https://doi.org/10.1061/(ASCE)AE.1943-5568.0000105.
[44] Caruso M, Pinho R, Bianchi F, Cavalieri F, Teresa M. A Life Cycle Framework for the Identification of Optimal Building Renovation Strategies Considering Economic and Environmental Impacts. Sustainability 2020:26.
[45] NTC. Norme Technice Per Le Costruzioni; 2018.
[46] Cosenza E, Del Vecchio C, Di Ludovico M, Dolce M, Moroni C, Prota A, et al. The Italian guidelines for seismic risk classification of constructions: technical principles and validation. Bull Earthq Eng 2018;16:5905–35. https://doi.org/10.1007/s10518-018-0431-8.
[47] Fajfar P. A Non-linear Analysis Method for Performance-Based Seismic Design. Earthq Spectra 2000;16:573–92. https://doi.org/10.1193/1.1586128.
[48] FEMA. Seismic Performance Assessment of Buildings, Volume 1 – Methodology, Second Edition. Washington D.C.: Federal Emergency Management Agency; 2018.
[49] FEMA. Seismic Performance Assessment of Buildings, Volume 3 – Supporting Electronic Materials and Background Documentation, Third Edition. Washington D.C.: Federal Emergency Management Agency; 2018.
[50] FEMA. Seismic Performance Assessment of Buildings, Volume 2 – Implementation Guide, Second Edition. Washington D.C.: Federal Emergency Management Agency; 2018.
[51] FEMA. Seismic Performance Assessment of Buildings, Volume 4 – Methodology for Assessing Environmental Impacts. Washington D.C.: Federal Emergency Management Agency; 2018.
[52] Günay S, Mosalam KM. PEER Performance-Based Earthquake Engineering Methodology. Revisited J Earthq Eng 2013;17:829–58. https://doi.org/10.1080/13632469.2013.787377.
[53] British Standards Institution. BS EN ISO 14040: Environmental Management - Life Cycle Assessment Principles and Framework. British Standards Institution; 2006.
[54] British Standards Institution. BS EN ISO 14044:2006+A1:2018 Environmental management - Life Cycle assessment - Requirements and guidelines. British Standards Institution; 2018.
[55] Simonen K, Huang M, Aicher C, Morris P. Embodied carbon as a proxy for the environmental impact of earthquake damage repair. Energy Build 2018;164:131–9. https://doi.org/10.1016/j.enbuild.2017.12.065.
[56] Chhabra JPS, Hasik V, Bilec MM, Warn GP. Probabilistic Assessment of the Life-Cycle Environmental Performance and Functional Life of Buildings due to Seismic Events. J Archit Eng 2018;24:04017035. https://doi.org/10.1061/(ASCE)AE.1943-5568.0000284.
[57] Menna C, Asprone D, Jalayer F, Prota A, Manfredi G. Assessment of ecological sustainability of a building subjected to potential seismic events during its lifetime. Int J Life Cycle Assess 2013;18:504–15. https://doi.org/10.1007/s11367-012-0477-9.
[58] Welsh-Huggins S, Liel A. Integrating hazard-induced damage and environmental impacts in building life-cycle assessments. In: Furuta H, Frangopol D, Akiyama M, editors. Life-Cycle Struct. Syst., CRC Press; 2014, p. 574–81. https://doi.org/10.1201/b17618-82.
[59] Welsh-Huggins SJ, Liel AB. Is a Stronger Building also Greener? Influence of Seismic Design Decisions on Building Life-Cycle Economic and Environmental Impacts. In: Bakker J, Frangopol DM, van Breugel K, editors. Life-Cycle Eng. Syst. 1st ed,. CRC Press; 2016. p. 975–82. https://doi.org/10.1201/9781315375175-123.
[60] Welsh-Huggins SJ, Liel A. A life-cycle framework for integrating green building and hazard-resistant design: examining the seismic impacts of buildings with green roofs. Struct Infrastruct Eng 2017;13:19–33. https://doi.org/10.1080/15732479.2016.1198396.
[61] Huang M, Simonen K. Comparative Environmental Analysis of Seismic Damage in Buildings. J Struct Eng 2020;146:05019002. https://doi.org/10.1061/(ASCE)ST.1943-541X.0002481.
[62] Simonen K, Merrifield S, Almufti I, Strobel K, Tipler J. Integrating Environmental Impacts as Another Measure of Earthquake Performance for Tall Buildings in High Seismic Zones. Struct. Congr. 2015, Portland, Oregon: American Society of Civil Engineers; 2015, p. 933–44. https://doi.org/10.1061/9780784479117.080.
[63] Arroyo D, Ordaz M, Teran-Gilmore A. Seismic Loss Estimation and Environmental Issues. Earthq Spectra 2015;31:1285–308. https://doi.org/10.1193/020713EQS023M.
[64] Belleri A, Marini A. Does seismic risk affect the environmental impact of existing buildings? Energy Build 2016;110:149–58. https://doi.org/10.1016/j.enbuild.2015.10.048.
[65] Dong Y, Frangopol DM. Performance-based seismic assessment of conventional and base-isolated steel buildings including environmental impact and resilience: Seismic Assessment Including Environmental Impact and Resilience. Earthq Eng Struct Dyn 2016;45:739–56. https://doi.org/10.1002/eqe.2682.
[66] Yang Y, Ingwersen WW, Hawkins TR, Srocka M, Meyer DE. USEEIO: A new and transparent United States environmentally-extended input-output model. J Clean Prod 2017;158:308–18. https://doi.org/10.1016/j.jclepro.2017.04.150.
[67] Sassun K, Sullivan TJ, Morandi P, Cardone D. Characterising the in-plane seismic performance of infill masonry. Bull N Z Soc Earthq Eng 2016;49:98–115. https://doi.org/10.5459/bnzsee.49.1.98-115.
[68] Cardone D. Fragility curves and loss functions for RC structural components with smooth rebars. Earthq Struct 2016;10:1181–212. https://doi.org/10.12989/EAS.2016.10.5.1181.
[69] Säynäjoki A, Heinonen J, Junnonen J-M, Junnila S. Input–output and process LCAs in the building sector: are the results compatible with each other? Carbon Manag 2017;8:155–66. https://doi.org/10.1080/17583004.2017.1309200.
[70] Majeau-Bettez G, Strømman AH, Hertwich EG. Evaluation of Process- and Input–Output-based Life Cycle Inventory Data with Regard to Truncation and Aggregation Issues. Environ Sci Technol 2011;45:10170–7. https://doi.org/10.1021/es201308x.
[71] Bare J. TRACI 2.0: the tool for the reduction and assessment of chemical and other environmental impacts 2.0. Clean Technol Environ Policy 2011;13:687–96. https://doi.org/10.1007/s10098-010-0338-9.
[72] US Bureau of Labour Statistics. CPI Inflation Calculator. US Bur Labour Stat; 2021. https://www.bls.gov/data/inflation_calculator.htm [accessed February 11, 2021].
[73] Carofilis W, Clemett N, Gabbianelli G, O'Reilly G, Monteiro R. Influence of parameter uncertainty in multi-criteria decision-making when identifying optimal retrofitting strategies for RC buildings. J. Earthquake Eng. 2021 [Under Review].
[74] Prota A, Di Ludovico M, Del Vecchio C, Menna C. Progetto DPC-ReLUIS 2019-2021 WP5: Interventi di rapida esecuzione a basso impatto ed integrati. RELUIS; 2020.
[75] McKenna F, Scott MH, Fenves GL. Non-linear Finite-Element Analysis Software Architecture Using Object Composition. J Comput Civ Eng 2010;24:95–107. https://doi.org/10.1061/(ASCE)CP.1943-5487.0000002.
[76] O'Reilly GJ, Sullivan TJ. Modeling Techniques for the Seismic Assessment of the Existing Italian RC Frame Structures. J Earthq Eng 2019;23:1262–96. https://doi.org/10.1080/13632469.2017.1360224.
[77] Crisafulli FJ, Carr AJ, Park R. Analytical modelling of infilled frame structures. Bull N Z Soc Earthq Eng 2000;33. https://doi.org/10.5459/bnzsee.33.1.30-47.
[78] Hak S, Morandi P, Magenes G, Sullivan TJ. Damage Control for Clay Masonry Infills in the Design of RC Frame Structures. J Earthq Eng 2012;16:1–35. https://doi.org/10.1080/13632469.2012.670575.
[79] Decanini LD, Liberatore L, Mollaioli F. Strength and stiffness reduction factors for infilled frames with openings. Earthq Eng Eng Vib 2014;13:437–54. https://doi.org/10.1007/s11803-014-0254-9.
[80] Carofilis W, Perrone D, O'Reilly GJ, Monteiro R, Filiatrault A. Seismic retrofit of existing school buildings in Italy: Performance evaluation and loss estimation. Eng Struct 2020;225:111243. https://doi.org/10.1016/j.engstruct.2020.111243.
[81] O'Reilly GJ, Perrone D, Fox M, Monteiro R, Filiatrault A. Seismic assessment and loss estimation of existing school buildings in Italy. Eng Struct 2018;168:142–62. https://doi.org/10.1016/j.engstruct.2018.04.056.
[82] Nafeh AMB, O'Reilly GJ, Monteiro R. Simplified seismic assessment of infilled RC frame structures. Bull Earthq Eng 2020;18:1579–611. https://doi.org/10.1007/s10518-019-00758-2.
[83] O'Reilly GJ, Sullivan TJ. Probabilistic seismic assessment and retrofit considerations for Italian RC frame buildings. Bull Earthq Eng 2018;16:1447–85. https://doi.org/10.1007/s10518-017-0257-9.
[84] Milanesi RR, Hemmat M, Morandi P, Totoev Y, Rossi A, Magenes G. Modelling strategies of ductile masonry infills for the reduction of the seismic vulnerability of r.c. frames n.d.:31.
[85] Priestley MJN, Calvi GM, Kowalsky MJ. Displacement-Based Seismic Design of Structures. 2nd ed. Pavia: EUCENTRE; 2017.
[86] Shafaei J, Nezami SA. Effect of different size of joint enlargement on seismic behavior of gravity load designed RC beam-column connections. Struct Des Tall Spec Build 2019;28. https://doi.org/10.1002/tal.1653.
[87] CEN. EN 1998-3 (English): Eurocode 8: Design of structures for earthquake resistance - Part 3: Assessment and retrofitting of buildings; 2005.
[88] Filippou FC, Popov EP, Bertero VV. Effects of bond deterioration on hysteretic behaviour of reinforced concrete joints.pdf. University of California Berkley; 1983.
[89] Collins MP, Denis M. Prestressed Concrete Structures. 1st ed. Ontario, Canada: Response Publications; 1997.
[90] Mander JB, Priestley MJN, Park R. Theoretical Stress-Strain Model for Confined Concrete. J Struct Eng 1988;114:1804–26. https://doi.org/10.1061/(ASCE)0733-9445(1988)114:8(1804).
[91] Mackie KR, Stojadinović B. Comparison of Incremental Dynamic, Cloud, and Stripe Methods for Computing Probabilistic Seismic Demand Models. Struct. Congr. 2005, New York, New York, United States: American Society of Civil Engineers; 2005, p. 1–11. https://doi.org/10.1061/40753(171)184.
[92] O'Reilly GJ, Sullivan TJ. Quantification of modelling uncertainty in existing Italian RC frames. Earthq Eng Struct Dyn 2018;47:1054–74. https://doi.org/10.1002/eqe.3005.
[93] Baker JW. Efficient Analytical Fragility Function Fitting Using Dynamic Structural Analysis. Earthq Spectra 2015;31:579–99. https://doi.org/10.1193/021113EQS025M.
[94] Silva A, Castro JM, Monteiro R. A rational approach to the conversion of FEMA P-58 seismic repair costs to Europe. Earthq Spectra 2020:875529301989996. https://doi.org/10.1177/8755293019899964.
[95] Porter K, Farokhnia D, Vamvatsikos D, Cho I. Guidelines for component based analytical vulnerability assessment of buildings and nonstructural elements. Pavia, Italy: GEM Foundation; 2014.
[96] Blengini GA. Life cycle of buildings, demolition and recycling potential: A case study in Turin. Italy Build Environ 2009;44:319–30. https://doi.org/10.1016/j.buildenv.2008.03.007.
[97] Hamilton P. How to estimate the cost of highrise cast-in-place flat slab construction; 2015.
[98] Hofstadler C. Calculation of construction time for building projects – Application of the Monte Carlo method to determine the period required for shell construction works. Proc 18th CIB World Build Congr, Salford, United Kingdom 2010.